Modeling and Evaluation of Aerial Layer Communications System Architectures

by

Stephen P Ajemian
B.S. Electrical Engineering
The Johns Hopkins University, 2004
M.S. Electrical Engineering
The Johns Hopkins University, 2008

Submitted to the System Design and Management Program
in Partial Fulfillment of the Requirements for the Degree of
Master of Science in Engineering and Management
at the
Massachusetts Institute of Technology

September 2013

Signature of Author:_____
Stephen Ajemian
System Design and Management Program

Certified by:_____
Bruce Cameron
Lecturer of Engineering Systems
Thesis Supervisor

Accepted by:_____
Patrick Hale
Director
System Design and Management Fellows Program

(THIS PAGE INTENTIONALLY LEFT BLANK)

Modeling and Evaluation of Aerial Layer Communications System Architectures

by

Stephen Ajemian

Submitted to the System Design and Management Program on 7/12/2013 in Partial Fulfillment of the Requirements for the Degree of Master of Science in Engineering and Management

Abstract

Airborne networks are being developed to provide communications services in order to augment space-based and terrestrial communications systems. These airborne networks must provide point to point wireless communications capabilities between aircraft and to ground-based users. Architecting airborne networks requires evaluating the capabilities offered by candidate aircraft to operate at the required altitudes to bridge communications among ground users dispersed over large geographic areas. Decision makers are often faced with choices regarding the type and number of aircraft to utilize in an airborne network to meet information exchange requirements. In addition, the type of radio required to meet user needs may also factor into the architecture evaluation for an airborne network. Aircraft and radio design choices must be made under cost constraints in order to deliver capable communications architectures at an acceptable cost.

Evaluating communications architectures is often conducted with modeling and simulation. However, evaluations typically focus on specific network configurations and can become intractable when varying design variables such as aircraft and radio types due to the complexity of the trade space being analyzed. Furthermore, the growth in choices for design variables (such as additional aircraft types) can lead to enormous growth in the number of feasible candidate architectures to analyze.

The methodology developed and presented herein describes an approach for evaluating a large number of architecture combinations which vary on aircraft type and radio type for representative airborne networks. The methodology utilizes modeling and simulation to generate wireless communications performance data for candidate aircraft and radio types and enumerates a large trade space through a computational tool. The trade space is then evaluated against a multi-objective decision model to rapidly down-select to a handful of candidate architectures for more detailed analysis.

The results of this analysis provide effective tools for reducing the complex trade space to a tractable number of architectures to make an informed architectural decision with no prior articulation of preferences for performance measures. For the notional concept of operation analyzed, the number of feasible architectures was approximately 500,000 for each of the two

radio types examined. The decision model implemented reduced the feasible architectures to approximately 50 near-optimal architectures for each radio type. From this manageable set of near-optimal architectures, an analysis is conducted to evaluate marginal benefits versus cost to further reduce the candidate architectures to 3 architectures for each radio type. From these remaining architectures, detailed analysis and visualization can be conducted to aid decision makers in articulating preferences and identifying a single “best” architecture based on mission needs.

The enumeration of the trade space using the computational tool and multi-objective decision model is highly flexible to incorporating new constraints and generating new candidate architectures as stakeholder preferences become clearer. The trade space enumeration and decision model can be conducted rapidly to down-select large trade spaces to a tractable number of communications architectures to inform an architectural recommendation.

Thesis Supervisor: Bruce Cameron
Title: Lecturer of Engineering Systems

Table of Contents

List of Tables

List of Figures

Acknowledgements

Throughout my time in the Systems Design and Management (SDM) program, I have continued to be awed and inspired by the amazing talents of the people within the MIT community. I have been challenged more than I could have ever anticipated and express my gratitude for the knowledge I've obtained throughout this program, both personally and professionally. I am honored to have the privilege of experiencing both the intellectual challenges of the MIT experience and my amazing professors and classmates.

I would like to express my sincerest thanks to Dr. Bruce Cameron for his constant guidance and support on this thesis. His research in system architecture was the inspiration for this work and his expertise was invaluable in helping me to understand and navigate through a complex problem space. I want to express my appreciation for his time and effort in advising me, reviewing my work and helping me communicate a complex topic clearly. I would also like to thank him for providing me access to the talented people in the System Architecture Lab, Daniel Selva and Marc Sanchez, who were instrumental in steering me in the right direction for this analysis. Daniel and Marc exposed me to a rich set of tools and techniques that I can apply beyond the SDM program to simplify complex systems and impact high technology development efforts for my entire career. I would also like to thank Daniel for reviewing my thesis and providing his expertise in trade space enumeration and multi-objective optimization which not only strengthened this thesis, but also my understanding of these subjects.

I would also like to thank my employer, the MITRE Corporation, for providing me with the opportunity to attend the SDM Program.

Lastly, I would like to thank my loving wife and lifelong friend, Lyndsay, for her unwavering support throughout this entire program. Yes, I can come on a walk with you and Vinnie now.

The views expressed in this thesis are those of the author and do not reflect the views or the positions of the Department of Defense or the MITRE Corporation.

1 Introduction

There is increasing interest within the Department of Defense in augmenting terrestrial and satellite communications systems through the use of aircraft with wireless communications payloads. Aircraft carrying these communications systems operate at the "aerial layer" which refers to the region between terrestrial wired and wireless infrastructure (from fixed towers) to space-based satellite communications systems. The actual region is dependent on the achievable altitudes of aircraft being employed, ranging anywhere between several hundred feet above ground level to upwards of 50,000 or 60,000 feet above mean sea level. A variety of aircraft are being considered for the provision of aerial layer communications including various remotely-piloted aircraft (RPA) [1].

Butler, Creech and Anderson define an "airborne network" as a mobile ad hoc network (MANET) consisting of at least one airborne node utilizing a line of sight (LOS) communications system [16]. Evaluating the performance of communications aircraft operating at the aerial layer focuses on two measures of performance: aircraft to aircraft connectivity and coverage area to ground based communications systems. Airborne networks consist of multiple aircraft operating over potentially large geographic distances to bridge connectivity between ground-based nodes. These network topologies can consist of multiple hops to bridge ground-based nodes, levying a requirement on airborne networks to provide connectivity with a high link uptime. Furthermore, airborne networks must also service mobile ground users dispersed over wide geographic areas having information exchange requirements that must be met in the presence of irregular terrain which limits LOS to the terrestrial and space-based communications infrastructure.

A notional depiction of an airborne network used to provide wireless communications is shown in Figure 1. The "users" of the airborne network depicted are the ground vehicles and users located in the command and control centers.

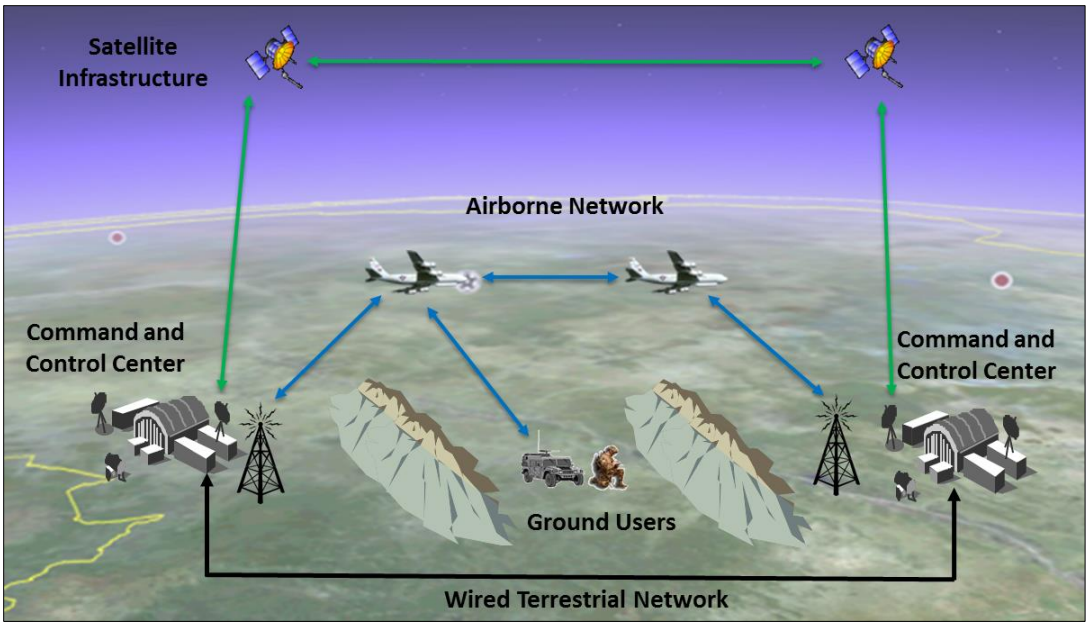

Figure 1. Example Airborne Network Use Case

The links in blue depict an airborne network which can be evaluated based on the measures of performance mentioned above. An example point to point connectivity evaluation could consist of the quality of the link between the two aircraft depicted. The link indicating connectivity to ground users must be evaluated for ground users operating over a large geographic area, so this performance measure must examine connectivity over the entire region for which an aircraft could provide connectivity to ground users.

Modeling and simulation plays a crucial role in evaluating predicted performance of aerial layer architectures and can be leveraged to inform decision making on building effective system architectures. Communications models of wireless systems are useful in analyzing the respective performance measures described above. However, these models are most effective for analyzing specific airborne network configurations with known quantities of aircraft providing communications operating at known locations. Trade space exploration can be difficult with existing tools as design variables (such as aircraft types) change. Candidate aircraft are constrained by limited capacity for payloads and achievable altitudes for providing communications to ground-based users. Because of the range of capabilities offered by candidate aircraft, multiple aircraft types are often considered for system architectures.

Maximizing performance of aerial layer communications at a system level can quickly become difficult as various aircraft types are introduced as candidates. Furthermore, evaluating multiple types of wireless communications systems for these architectures introduces more complexity into the architectural decision. The growth of design variables in the architectural decision poses challenges to system architects to develop capable system architectures at an acceptable cost as the number of candidate architectures grows. Existing tools can be extended to evaluate candidate architectures over a range of design decisions to provide the insight needed to develop optimal system architectures.

2 Motivation

As stated in Chapter 1, the users of the airborne network consist of mobile ground vehicles operating on-the-move or command and control centers in a fixed location. Designing aerial layer architectures to service these users will focus on the measures of performance presented above: point-to-point connectivity among aircraft and coverage area to ground-based vehicles. Ground vehicles pose significant challenges for closing wireless links as they are subject to frequent outages due to line of sight blockages due to irregular terrain. These outages are exacerbated by the limited antenna height on ground vehicles, inducing frequent terrain blockage.

Evaluating communications system architectures aimed at maximizing point-to-point connectivity and connectivity to ground vehicles through airborne networks with radio frequency (RF) propagation models is computationally intensive. Candidate aircraft have the potential to cover large geographic areas because of the altitudes these aircraft can achieve. To understand the effects of altitude on computation time, LOS distance is a crude measure that can be utilized to calculate the maximum coverage area that an aircraft can provide and represents the longest distance the asset can see over curved earth. This distance is referred to as the radio horizon, and is given by the following equation:

$$Radio\ Horizon_{km} \approx 1.61 * \sqrt{2 * Altitude_{feet}} \quad (1)$$

Table 1 shows the radio horizon for various altitudes. These distances represent the maximum propagation distance of a wireless link. Ground coverage computations for aircraft operating at these altitudes must include all points on the ground within the radio horizon. The number of ground points that must be evaluated grows substantially as altitude increases and significantly lengthens computation time for analysis aimed at evaluating performance over the entire geographic region covered by aircraft.

Table 1. Radio Horizon for Various Altitudes

Altitude (ft)	Radio Horizon (km)
1,000	72
10,000	228
20,000	322
30,000	394
40,000	455
50,000	509

Analyzing RF propagation for communication systems integrated on aircraft must evaluate link performance over large geographic areas for each individual aircraft servicing ground users. The design of aerial layer architectures can potentially consider multiple aircraft types operating at various altitudes as a design variable. In addition, the number of aircraft being employed in the architecture can vary as well, as decision makers often require insight into the marginal benefits of the aerial layer architecture as more aircraft are added. Evaluating candidate architectures quickly becomes difficult as the number of assets grows and various aircraft types are introduced for hosting communications payloads.

Prior to the evaluation of aerial layer communications architectures, an understanding of the number of feasible candidate architectures is required. Several assumptions are made in this analysis on aircraft types and the number of aircraft under consideration. For this analysis, a predetermined number of aircraft are assumed to operate over several fixed sites in a representative scenario chosen by the author. The number of sites being considered for augmentation with an aircraft hosting a communications system is 12 sites and two aircraft are considered as host aircrafts for the radio system. At each site, the decision to be made consists of selecting one of the two aircraft, or neither aircraft, for a total of three choices (1 plus the number of aircraft types). This decision is made at all 12 sites, so the number of combinations of candidate architectures grows quickly as more sites or more aircraft are considered. The total number of combinations of candidate architectures is given by the following equation (where N_i is the number of aircraft types at site i and N_S is the number of candidate sites):

$$\text{Candidate Architectures} = \prod_{i=1}^{N_S} (N_i + 1) \tag{2}$$

For the case of $N_i = 2$ and $N_S = 12$, there are 531,441 architectures for a single radio type. If two radios are considered separately, this doubles the number of candidate architectures to 1,062,882. It should be noted that homogeneous radio architectures are assumed where only one radio type is employed for a given deployment. Such a large number of architectures introduces substantial complexity into the architectural decision process and raises challenges for conducting detailed performance analysis.

Performing detailed link analysis using propagation models for this number of architectures is infeasible given the complexity of this performance evaluation. Furthermore, as more candidate aircraft are considered, the number of combinations to analyze is further increased. This complexity of the trade space can pose significant challenges for system architects to identify optimal architectures or to differentiate among a large number of options. Prioritizing performance requirements in aerial layer communications architectures can be both difficult and subjective for system architects as well, making the architecture evaluation even more challenging.

The motivation for this thesis is to develop a methodology for identifying communication system architectures that optimize performance across several performance domains through enumeration of the entire trade space and applying a multi-objective optimization algorithm to yield a range of optimal candidate architectures. From this range of options, decision makers can make tradeoffs within a manageable set of candidate solutions, simplifying the architectural decisions of aircraft types, radio types and the number of aircraft/radio pairs to deploy. In addition, this methodology will evaluate candidate architectures based on cost so decision makers can select the lowest cost architectures achieving the desired communications performance of aerial layer architectures. The use of modeling and simulation to conduct an architecture evaluation is a cost-effective way of rapidly selecting optimal architectures from a large number of candidates.

Communications models representing aerial layer communications cannot represent every real-world condition or attributes encountered in building airborne networks due to the inherent complexity of the problem space. Propagation models cannot account for every variable encountered in real-world systems that can degrade performance (such as foliage, urban terrain, or small-scale fading conditions). However, these limitations are outweighed by the insights that can be gleaned from high-fidelity models to answer architectural questions without incurring the costs of having to build and test actual systems.

3 Methodology

3.1 Literature Review

Extensive research has been conducted in trade space exploration of system architectures based on the identification of user needs. In [17], Cameron, Crawley and Selva examine system architecting decisions by framing an architecture decision broadly as an optimization problem. Such optimization problems can be solved computationally; however care must be taken when formulating such optimization problems. For cases where design variables do not take real values, but rather a set of integer values, the optimization problem becomes a combinatorial optimization problem which is NP-hard [17]. In such cases, system architects must scope the number of decisions appropriately as the trade space increases exponentially as the number of decisions increases. The delivery of value to stakeholders can be defined by one or more value functions, implying that value delivery to stakeholders is multi-objective. Such multi-objective optimizations make the discovery of a single "optimal" architecture infeasible, but rather return a Pareto front of non-dominated architectures [17]. Evaluating a Pareto front for deciding candidate system architectures can be subjective in the absence of a priority of value functions and ambiguous user needs. As was discussed in 2, the architecting of an airborne network can be framed as a combinatorial optimization problem consisting of various aircraft types operating at certain altitudes. In addition, radio systems and aircraft types can be evaluated in terms of performance metrics. A computational tool is utilized for this architectural assessment to rapidly synthesize architectures in the optimization model taking as inputs performance metrics for individual aircraft.

Sanchez, Selva, Cameron and Crawley present a method for architectural trade space exploration in [14] for a large number of communications architectures. The trade space exploration is conducted through the enumeration of candidate architectures through a computational tool which also models the performance of candidate architectures. Performance metrics are derived from a stakeholder analysis and used as the basis of architecture down-selection after enumeration of the trade space. The enumeration of a large trade space of candidate architectures using a computational tool followed by down-selection

based on performance metrics can be an effective method for architecture evaluations consisting of a large trade space. For the enumeration of a trade space for aerial layer communication architectures, the use of a computational tool that can synthesize candidate architectures for optimization based on performance metrics can allow architects to quickly down-select the large search space to a manageable number of architectures. The application of an optimization model to generate a Pareto front for multi-objective performance metrics can reduce this trade space to a manageable set of architecture decisions.

Ross, Hastings, and Warmkessel describe a process in [15] in which an architecture level analysis is conducted based on a utility assessment derived from a set of user needs. The output of the architecture-level analysis is a Pareto front which is utilized for more detailed analysis. Applying high-fidelity analysis to a subset of candidate architectures (derived from the Pareto front) can provide time savings in development [15]. A similar approach is presented for this architectural assessment. An enumeration of the trade space is conducted computationally and a Pareto front is generated from a multi-objective optimization model. From this Pareto front, further analysis is applied to down-select to a handful of candidate architectures for high-fidelity modeling.

3.2 Enumeration and Evaluation of Candidate Architectures

The sequential process presented for modeling and evaluating communication architectures is summarized in Figure 2. Similar to the methodology presented in [14], a concept of operation is developed utilizing an aerial layer communications architecture. A representative scenario implementing the concept of operations is presented using two notional radio systems which will be evaluated against each other on several measures of performance, including cost. These radio systems will be hosted as payloads on two possible candidate aircraft with different performance capabilities and costs. A trade space will be enumerated for each radio system for various aircraft combinations and a set of near-optimal architectures will be selected utilizing a multi-objective optimization model. The optimal architectures will be obtained from the multi-objective optimization model which provides the basis of the architectural recommendation.

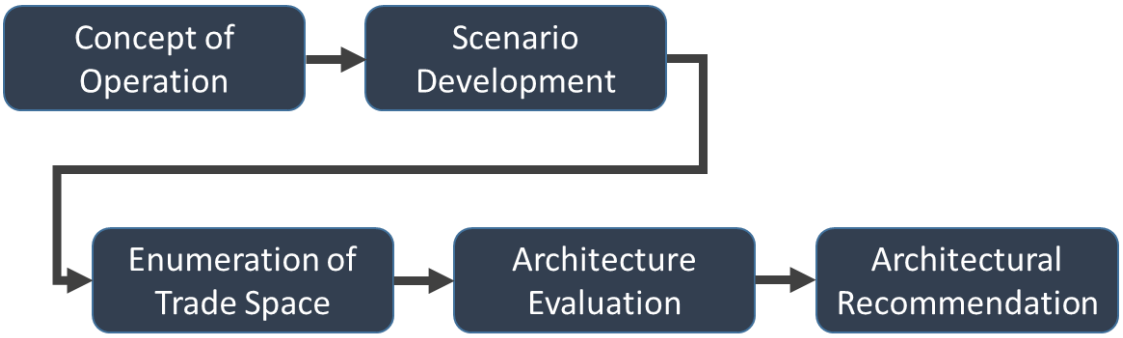

Figure 2. Communications Architecture Evaluation Methodology

The architectural recommendation consists of a subset of candidate architectures for which detailed analysis can be conducted. The architecture evaluation allows the down-selection to a tractable subset of architectures that can be further analyzed at higher levels of fidelity after which they can be presented to stakeholders to facilitate discovery of the relative weights of importance for the performance metrics used in the trade space enumeration.

4 Concept of Operation

The Department of Defense is investing heavily in Internet Protocol (IP) radio technologies to provide line of sight connectivity among aircraft [18]. The use of IP-based LOS communications systems has the potential to offer high-capacity links to augment satellite communications (SATCOM) systems. LOS communications systems can provide robust communications capabilities in situations where SATCOM links are stressed due to high user demand or offer degraded performance over severe terrain [19].

Military users cannot rely on wired terrestrial infrastructure to meet communications needs in sustained military conflicts. While SATCOM systems aim to provide global coverage to military users, the actual coverage and communications services offered in a specific region may not meet the service levels required for mission effectiveness. The use of airborne networks to augment SATCOM can improve mission effectiveness [16]. In addition to providing additional capacity, LOS communication systems offer lower latencies for information exchanges due to the shorter propagation distances over SATCOM alternatives.

The concept of operation for an aerial layer communications architecture to meet the operational need described above consists of integrating candidate wireless communications payloads on aircraft. It is assumed that the aircraft can host these candidate communications payloads and launch from the command and control centers requiring augmentation of communications infrastructure. The aircraft considered are assumed to provide the capability to loiter for a sufficient length of time to meet the operational need described above for the provision of wireless access to mobile ground vehicles and to other aircraft in the system architecture.

5 Scenario Development

For the purposes of evaluating aerial layer communications architectures with the intended methodology, a notional scenario is required to implement the concept of operations presented above. The scenario consists of hosting two competing radios on aircraft for performance evaluation. Two competing radio technologies are described which differ in the throughput offered, tolerable propagation loss, and cost. The performance parameters of these radio systems are representative of tactical military radios and will serve as realistic approximations of actual radio systems. Additionally, two aircraft are described which will serve as the candidate aircraft used in the exploration of the trade space. These aircraft differ in the achievable altitudes that they can loiter at, in addition to cost. Candidate architectures will consist of hosting radio and aircraft combinations at 12 sites located in the southwestern United States. This region was selected intentionally to emulate challenging terrain which can impose line-of-sight blockages on disadvantaged users and command and control centers.

5.1 Radio Systems

As stated above, the performance characteristics of the two radio systems being considered consist of propagation range and cost. These performance measures are incorporated quantitatively into the architecture evaluation. The candidate radios, Radio A and Radio B, are also assumed to differ in throughput in Megabits per second (Mbps). This metric describes the amount of data that the radio links can transmit and receive to service the information exchange requirements of users. However, throughput is not incorporated into the evaluation directly, but rather as a subjective measure to differentiate the final candidate architectures. The consideration of throughput is further described in Chapter 6. Extensions of the model to incorporate throughput directly are described in Chapter 11. The tactical radios are assumed to utilize time-division multiple access (TDMA). In TDMA, access to the channel for transmission and reception of messages is broken up into time slots. In a given time slot, a radio can either transmit or receive. This has implications for throughput for two nodes connected through relay nodes. In such cases, total throughput is cut in half as the relay nodes cannot transmit in the same time slot they are receiving in. Degradation of throughput for relay cases has

implications for desirable network architectures [20]. Architectures that maximize the number of nodes that can communicate directly are advantageous because throughput is less likely to be cut in half due to relay. This measure of performance is discussed further in 6.3.

The radio systems are assumed to be wireless communications systems that can only tolerate a threshold amount of propagation loss, given in decibels (dB). Tolerable path loss governs the range that these radio systems can reach and the amount of attenuation that can be tolerated due to propagation range and terrain obstructions. As wireless signals propagate over-the-air, the signal power degrades over distance. Propagation loss can be calculated using the free space path loss (FSPL) equation presented in [5], where d is the distance traveled in kilometers, and f is the frequency of operation in megahertz (MHz):

$$FSPL_{dB} = 20\log_{10}(d) + 20\log_{10}(f) + 32.45 \quad (3)$$

Signal power is further reduced when these waves propagate through terrain obstructions located between the transmitter and receiver. Additional attenuation due to terrain obstructions depends on the depth of the terrain that the signal is propagating through and propagation conditions could exist where the depth of blockage may not necessarily prevent link closure if sufficient link margin exists. The path loss computation accounting for the presence of terrain is described in 6.2.

The radio systems are defined to operate at similar frequencies within the L-band spectrum (1 to 2 GHz) and utilize the same antenna. Integrating radio systems on aircraft can reduce the performance of these systems as cabling between the radio and antennas impose additional RF losses. RF filters are often employed to reduce out of band signal emissions that could interfere with other co-located systems. These filters will also impose additional losses which degrade performance. Because these cable and filter losses are assumed to be the same for each radio system, these losses can be omitted with no loss of fidelity to the architectural evaluation. Attenuation varies over frequency, though for the purposes of comparison, performance

differences due to different operating frequencies will not factor into the analysis because they will operate on the same frequency. The L-band spectrum is frequently used for tactical communications systems, and represents a reasonable assumption for a communications system. A half-wave dipole antenna is assumed for each radio system, offering a peak gain of approximately 2 dB.

Radio A

Radio A is defined to be a low-cost tactical radio that can provide a throughput of up to 2 Mbps at a cost of $50,000 per radio. This radio is assumed to have a transmit power of 10 W and can "close" a radio link if the received signal power is above -90 decibel-milliwatt. This radio will operate in the L-band frequency spectrum and for the purposes of this analysis, the operating frequency will be 1350 Megahertz. A link budget is presented in Table 2 below to indicate the maximum tolerable path loss, assuming peak antenna gain of the dipole antenna.

Table 2. Radio A Tolerable Path Loss

Transmit Power	40.0	dBm
Antenna Gain (Transmit)	2.0	dB
Antenna Gain (Receive)	2.0	dB
Receiver Sensitivity	-90.0	dBm
Maximum Tolerable Path Loss	134.0	dB

Radio B

Radio B is defined to be higher-cost tactical radio that can provide throughput of up to 10 Mbps at a cost of $150,000 per radio. This radio is assumed to have a transmit power of 50 W and can close the radio link if the received signal power is above -95 decibel-milliwatt. This radio will also operate in the L-band frequency spectrum (1350 MHz). A link budget is presented in Table 3 below to indicate the maximum tolerable path loss, assuming peak antenna gain of the dipole antenna.

Table 3. Radio B Tolerable Path Loss

Transmit Power	47.0	dBm
Antenna Gain (Transmit)	2.0	dB
Antenna Gain (Receive)	2.0	dB
Receiver Sensitivity	-95.0	dBm
Maximum Tolerable Path Loss	146.0	dB

A summary of the performance of Radio A and Radio B is shown in Table 4 highlighting the key measures of performance utilized for architecture evaluations: throughput, tolerable path loss, and cost.

Table 4. Summary of Candidate Radio Systems

Radio	Throughput (Mbps)	Tolerable Path Loss (dB)	Cost (Dollars)
Radio A	2	134.0	$50,000
Radio B	10	146.0	$150,000

5.2 Aircraft

The aircraft considered for this analysis are intentionally assumed to be generic aircraft with the capability to loiter at altitudes ranging from 1,500 to 3,000 feet above ground level. The two aircraft presented are assumed to be capable of loitering in a stationary position at specific fixed sites throughout the duration of the communications mission described in the concept of operation. The static positions of the aircraft reduce the duration of the analysis substantially because the performance of radio systems will not vary over time.

Assumptions on the procurement costs of these aircraft types are made for the cost calculation. The aircraft cost can easily be extended to account for additional costs data such as lifecycle cost including personnel required to operate the aircraft, maintenance costs such as repairs, or additional equipment required to operate the aircraft, but they are omitted in this analysis. The intent of using procurement costs is to provide a relative cost difference between the two aircraft which offer different performance from the perspective of achievable altitude. This cost difference assumes that Aircraft 2 can loiter at an altitude twice as high as Aircraft 1, but costs twice as much. The assumption that these candidate aircraft are capable of loitering in a fixed

position allows for a static analysis to be completed for communications performance. Chapter 11 presents an approach to extending the model to account for dynamic aircraft traversing flight paths over time.

Aircraft 1

Aircraft 1 is assumed to be a less capable aircraft limited to loiter altitudes of 1,500 feet above ground level (AGL). Note that the radio horizon for this altitude (based on Equation 1) is approximately 88 km. The candidate radios are assumed to be hosted on the underside of the candidate aircraft with no antenna blockage effects imposed by the aircraft. The procurement cost of Aircraft 1 is assumed to be $5 million.

Aircraft 2

Aircraft 2 is assumed to be the more capable aircraft being considered in the architectural evaluation. It is assumed to be able to loiter at a height of 3,000 feet AGL which has a radio horizon of 125 km. The procurement cost of this aircraft is assumed to be $10 million. It is assumed that the radio systems are integrated on the underside of the aircraft and no aircraft blockage effects are imposed on the antennas for this analysis.

A summary of the Aircraft 1 and 2 systems is shown in below and will be the assumptions used in the architecture evaluation.

Table 5. Aircraft Assumptions

Aircraft	Loiter Altitude (ft AGL)	Procurement Cost (Dollars)
Aircraft 1	1500	$5 million
Aircraft 2	3000	$10 million

Mobile Ground Vehicle

The deployment of aircraft for communications extension is predominantly in support of "disadvantaged" nodes operating in challenging RF propagation conditions imposed by irregular

terrain, represented by a mobile ground vehicle integrated with a radio system. For the purposes of this analysis, a ground vehicle is employed with an antenna height of 10 feet above ground level. This node will be utilized for calculating area covered by a given aircraft deployment by acting as the receiving node for the coverage calculations. The cost of the ground vehicles integrated with the candidate radios is not considered in the evaluation because the number of vehicles needed is driven by specific mission needs and not assumed to be dependent on the coverage area provided by candidate architectures.

5.3 Communications Model

The Systems Toolkit (STK) communications analysis tool can be used to recreate the intended concept of operations described above with the airborne and ground vehicles aircraft integrated with Radio A and Radio B. The aircraft described above are implemented in the scenario at the requisite loiter altitudes and antenna heights to accurately model the geometries imposed on the RF transmissions.

5.3.1 Systems Tool Kit Overview

STK is a commercial off-the-shelf (COTS) computer application developed and marketed by Analytical Graphics, Incorporated. STK is a physics-based geometry engine that can display and evaluate performance of communications assets hosted on land, sea, air, and space assets in real or simulated time. These assets can be evaluated and visualized in 3-dimensional space to answer questions such as:

- Where are the communications nodes being modeled?
- What can the communications nodes see?
- When can the nodes see other nodes?

Wireless communication assets can be defined in STK based on physical-layer performance measures such as transmit power and receiver sensitivity and combined with RF propagation models incorporating line-of-sight blockages due to terrain. These RF models can calculate when, where and how well exchanges occur beyond simple line-of-sight visibility.

STK can assess the quality of spatial and communication relationships through a wide array of constraining conditions while also incorporating environmental factors such as terrain and weather conditions on sensor visibility or communication link quality. Performance assessments of modeled scenarios can be exported to a variety of reports and graphs summarizing performance over time. STK requires platform locations and their movement plan as a function of time in order to calculate the coverage area for a particular platform. Additionally, interference imposed on communications systems can be represented in STK to examine performance of communication systems in the presence of jamming due to adversaries or co-channel interference of other communications systems.

STK provides a variety of outputs including engineering parameters (such as link budget) and operational performance parameters (such as times, locations, or areas for which links are closed) which can be applied to the scenario defined in this analysis. Coverage regions from aircraft to ground nodes can be visualized through contour plots or through point-to-point connectivity between aircraft (as shown in Figure 3).

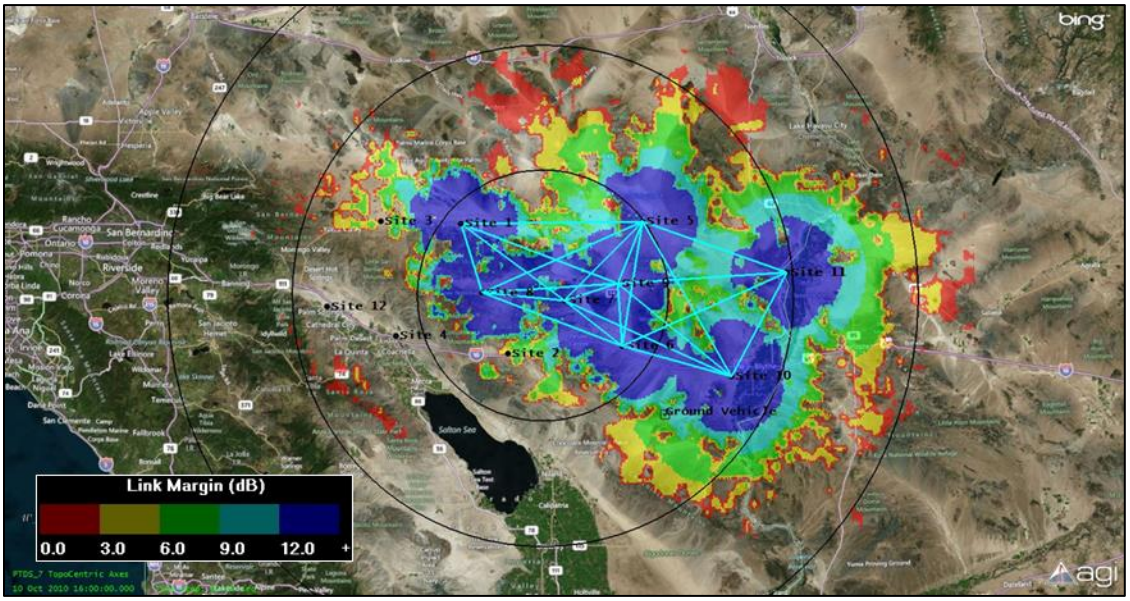

Figure 3. Sample of STK Graphical Output

The sample output shown above is a contour plot of link margin as a figure of merit for an example ground coverage computation. In this example, aircraft are placed at the candidate sites to evaluate link margin to a ground vehicle placed throughout the region. Greater link margin equates to better radio performance as it is a measure of received signal level seen at the receiver. Higher link margin can provide more reliable communications over wireless channels and can be utilized for extending this analysis to incorporate adaptive data rates for the radios considered.

Terrain Integrated Rough Earth Model

The Terrain Integrated Rough Earth Model (TIREM™) is an RF propagation software developed by Alion Science and Technology, Inc. used to predict RF performance of radio links over irregular terrain and bodies of water [4]. The TIREM path loss model can be incorporated into an STK scenario to dynamically assess propagation loss of candidate radio systems hosted on ground and aircraft. By incorporating digital terrain elevation data (DTED), RF propagation can be predicted with a sufficient level of fidelity over geographic regions featuring irregular terrain features. A discussion of the limitations of TIREM is presented in [4] describing additional factors that could affect path loss estimates that are not accounted for such as foliage and multipath effects. Additionally, statistics are provided for TIREM performance over several terrain profiles. The propagation model will calculate losses due to radio waves diffracting through terrain located between transmitters and receivers. RF propagation losses imposed on radio links due to atmospheric effects can be calculated as well. The capability of TIREM to predict RF propagation performance over irregular terrain makes it appropriate for modeling the performance of the wireless architectures posed in this analysis. Further information on the TIREM path loss model is available in [4].

5.3.2 Deployment Scenario

The location for a representative deployment of aircraft for communications relay missions was selected to intentionally incorporate mountainous terrain to create challenging propagation environments for ground vehicles representing the disadvantaged nodes and terrain blockages

imposed on aircraft to aircraft communications. A region located around Palm Springs, California is utilized for the 12 site laydown shown in Figure 4. The coordinates for each site are shown in Table 6 below.

Table 6. Site Locations

Site Number	Latitude	Longitude
Site 1	34.136558	-115.903086
Site 2	33.669871	-115.705213
Site 3	34.146973	-116.248642
Site 4	33.735752	-116.185912
Site 5	34.136799	-115.120283
Site 6	33.692386	-115.21614
Site 7	33.857772	-115.460889
Site 8	33.888899	-115.813875
Site 9	33.916066	-115.230627
Site 10	33.576399	-114.748968
Site 11	33.945486	-114.501989
Site 12	33.842098	-116.482938

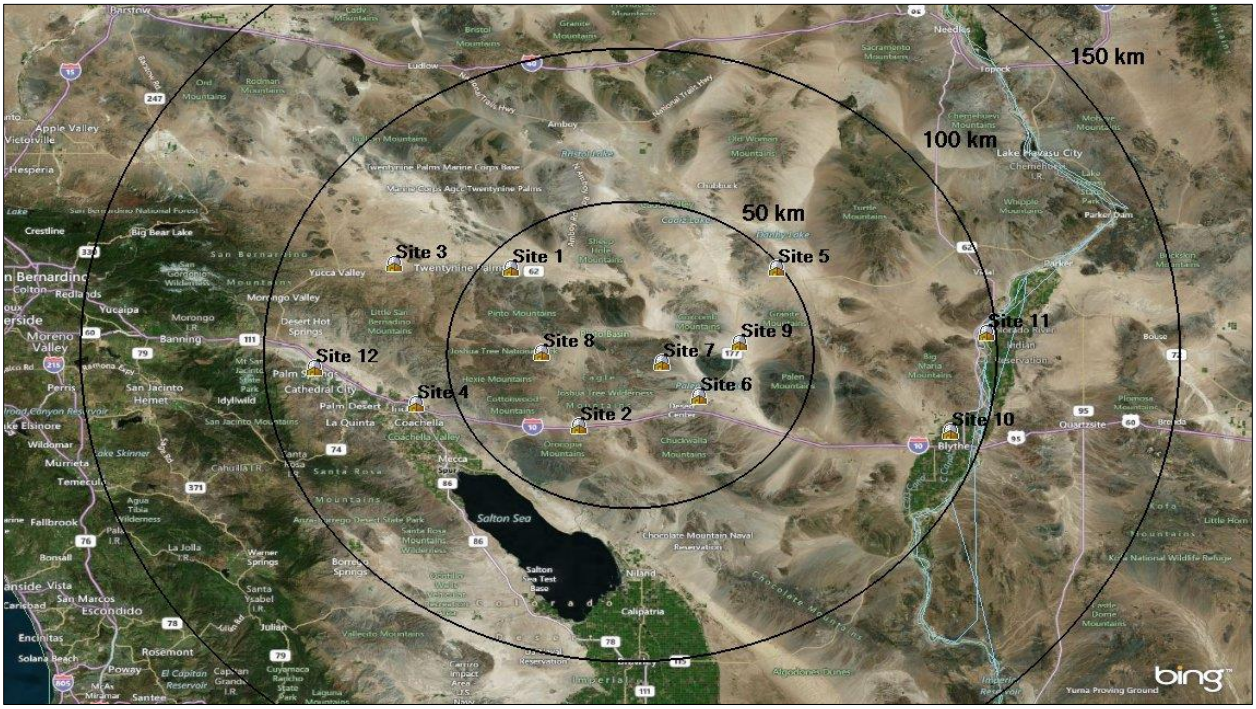

Figure 4. Deployment Scenario Modeled in STK

A 3-D view is shown in Figure 5 below to illustrate the mountainous terrain in this region which will impose challenging geography for closing the RF links modeled for Radio A and Radio B. This vantage point is taken from Aircraft 2 at Site 10 looking west towards other potential deployment sites. The use of DTED data allows for irregular terrain to be imported into the path loss computations using TIREM. Terrain blockages will typically prevent radio links from closing unless there is sufficient link margin to overcome the attenuation of the radio signal or the radio links in a point-to-point link calculation have sufficient altitude above ground level to overcome terrain obstructions.

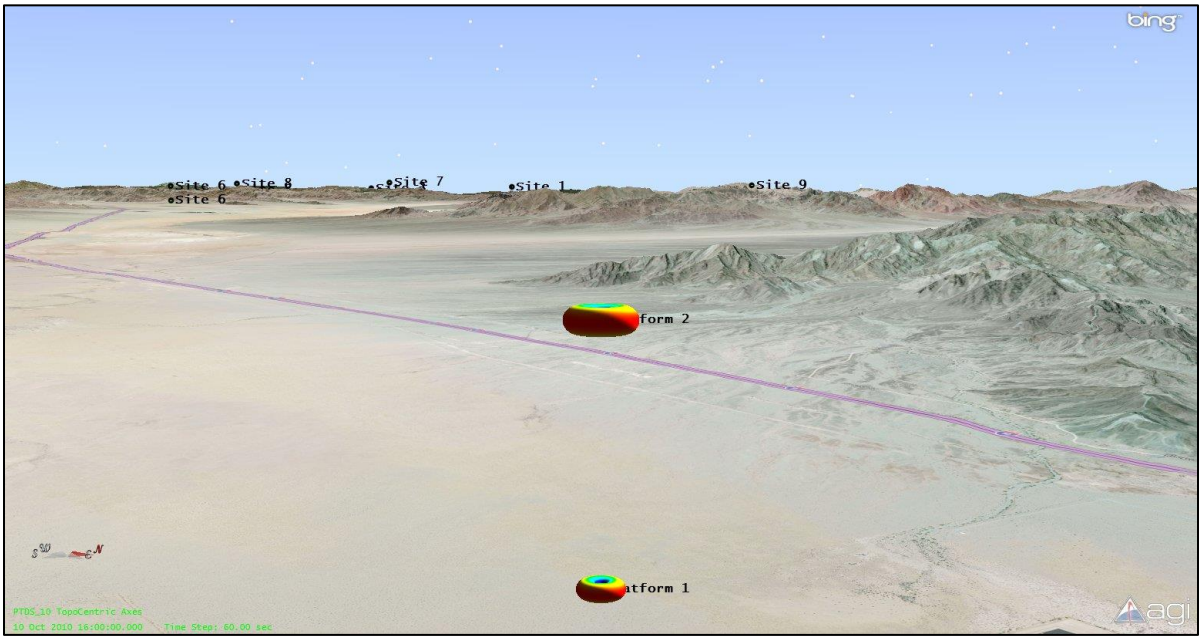

Figure 5. 3-D View of Local Terrain from Site 10

5.3.3 Aircraft Model

When integrating antennas on actual aircraft, the performance of the link can degrade due to obstructions imposed on the antenna by the host aircraft. The model ignores potential obstructions imposed on antennas integrated on the aircraft due to additional equipment or from the host aircraft, though STK provides the capability to calculate masking of the antenna due to these effects if a 3-D model of the aircraft is provided. To model the respective altitude heights, each aircraft is placed at 1,500 feet or 3,000 feet AGL, depending on the aircraft type.

Antennas are oriented at these heights for the modeling of RF propagation. A view of the aircraft implementation is shown in Figure 6 below with the dipole antenna pattern described above.

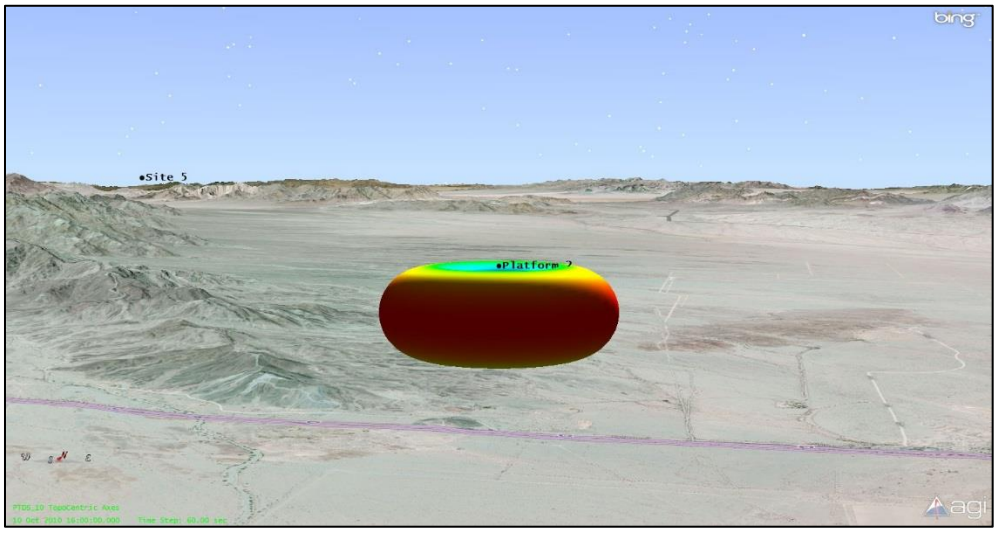

Figure 6. Aircraft with Dipole Antenna

5.3.4 Mobile Ground Vehicle Model

The mobile ground vehicle assumes the same dipole antenna employed on the aircraft at a height of 10 feet above ground level. A view of the STK implementation is shown below in Figure 7 of the ground vehicle and antenna radiation pattern. This ground vehicle is used as the receiving link in the ground coverage computations for Radio A and Radio B described in subsequent sections.

Figure 7. Mobile Ground Vehicle with Dipole Antenna

6 Architectural Decision Strategy

The primary decisions for deploying the aforementioned communications system architecture consists of which aircraft to deploy at each site (Aircraft 1, Aircraft 2 or none) and the radio system (Radio A or Radio B) to be utilized for the deployment, which is assumed to be used universally – mixed radio scenarios are not modeled, because the radios are not interoperable. Therefore, a mix of both types is not allowed in a given candidate architecture. The analysis will perform two architecture evaluations, one for each radio type and a comparison will be conducted on the overall performance of each radio type for the final candidate architectures selected. The architectural decisions are summarized in Table 7.

Table 7. Architectural Decisions

Decision	**Options**	**Total Number of Options**
Number of aircraft to deploy (N_D) to given number of sites (N_S)	Up to N_{Sites}	N_{Sites} (≤12 sites)
Payload	Radio A or Radio B	2
Aircraft	Aircraft 1, Aircraft 2 or none	3

In order to evaluate the optimal deployment strategy of candidate radios and aircraft, several measures of performance must be examined based on user needs. At a high-level, these measures of performance consist of total coverage area for ground vehicles, the average number of point-to-point radio links that can be closed, and the total cost of the architecture.

The ground coverage measure of performance will provide decision makers with knowledge of the total coverage footprint to ground vehicles over the geographic area being analyzed. Because ground vehicles requiring communications services could potentially operate over a wide geographic region, this measure of performance will quantify the coverage footprint over the deployment region.

Site-to-site connectivity is employed as both a measure of throughput performance and a measure of network resilience to the absence of aircraft due to downtime, which is described in [16] as a network characteristic impacting performance. By maximizing the average number of point-to-point links, or "crosslinks", throughput performance of radio systems can be increased by minimizing the number of relays. Relaying data typically cuts throughput in half, as a transmitting radio cannot typically receive while transmitting [20]. This measure will quantify the performance of the network topology for a given candidate architecture in this regard. In addition, the site-to-site connectivity measure will quantify network resilience to the loss of aircraft not able to operate on a given communications mission. This performance metric is applicable to decision makers because aircraft are unlikely to have 100% availability. A discussion of the suitability of site-to-site connectivity as a network resilience measure will be presented in 10.2 as it applies to the final candidate architectures. A summary of the performance outputs are provided in Table 8.

Table 8. Performance Outputs

Output	**Units**	**Tools Used**
Ground Coverage Area	Area in km^2	STK/MATLAB
Site-to-Site Connectivity (average number of crosslinks)	Dimensionless	STK/MATLAB
Architecture Cost	Total Cost for deploying N_{Deploy} Aircraft and Payloads	MATLAB Multi-Objective Decision Model

In order to evaluate the performance outputs described in Table 8, an intermediate dataset is generated offline using STK. This dataset consists of the individual communications performance metrics for each of the 24 aircraft being considered. These intermediate performance outputs are summarized in Table 9 and consist of link margin computations obtained from the STK model for both ground coverage performance and site-to-site connectivity. The dataset generated offline is used as an input to the MOO model implemented using the multi-objective genetic algorithm function in MATLAB.

Table 9. Intermediate Performance Outputs

Output	Units	Tools Used
Ground Coverage Area	Maximum Link Margin from each aircraft (in dB) to ground vehicle	STK
Site-to-Site Connectivity	Link Margin (in dB) to/from Sites	STK

A process flow for the architecture evaluation is illustrated in Figure 8 highlighting the use of STK to generate the intermediate dataset utilized in the MOO model. The performance outputs listed in Table 8 are generated during the execution of gamultiobj. Note that the details of the gamultiobj used in the MOO model to iteratively generate candidate architectures and identify optimal architectures is omitted from this process flow for simplicity. The intent of this process flow is to illustrate the generation of intermediate data in STK utilized by the MOO model to generate system-level performance of candidate architectures.

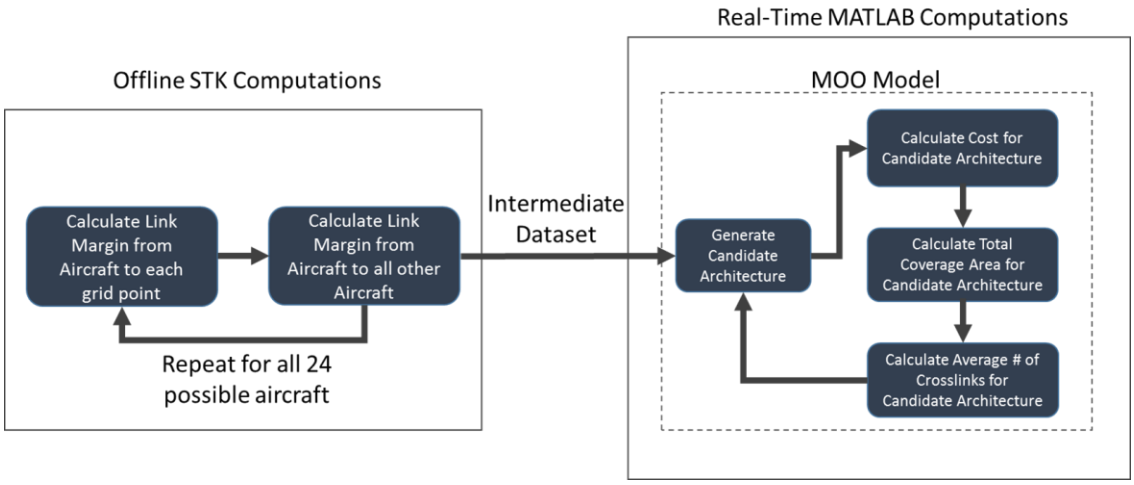

Figure 8. Process Flow for Architecture Evaluation

6.1 Architecture Cost

The cost computation that will be utilized will consist of the aircraft costs described above for the respective aircraft plus the costs for deploying a candidate radio at each site. The ground vehicle cost is not considered in the computation. For a given site, the cost will be computed by the following equation:

$$Site\ Cost = Aircraft\ Cost + Radio\ Cost \tag{4}$$

where the total architecture cost is the sum of all site costs for a given deployment of a radio system:

$$Architecture\ Cost = \sum_{i=1}^{N_D} Site\ Cost_i \tag{5}$$

The cost function increases linearly as more sites are added because there is a fixed cost for each radio/aircraft pair deployed at a given site.

6.2 Ground Coverage

Ground coverage performance consists of measuring the link margin in dB for a given radio link from the aircraft to the ground vehicle. For a ground vehicle at a given point, the link margin must be computed to this receiver from all aircraft in a given candidate architecture. This computation will utilize the TIREM path loss model at 1350 MHz, incorporating free space path loss, atmospheric losses, and terrain losses, in addition to the transmitter and receiver performance from the candidate radios. A single computation from a transmitter on an aircraft to a receiver on a ground vehicle is obtained from the following equation:

$$\begin{aligned} Link\ Margin_{dB} = {} & Transmit\ Power_{dBm} + Transmitter\ Gain_{dB} - TIREM\ \ Losses_{dB} + \\ & Receiver\ Gain_{dB} - Receiver\ Sensitivity_{dBm} \end{aligned} \tag{5}$$

where TIREM losses are given by the following expression:

$$TIREM\ \ Losses_{dB} = FSPL_{dB} + Atmospheric\ Losses_{dB} + Terrain\ Losses_{dB} \tag{6}$$

Note that the receiver sensitivity for a given radio will be either -90 dBm or -95 dBm, depending on the radio link being computed. The antenna gain for a given transmit/receive computation will vary depending on the look angles imposed by the geometry of the transmit/receive pair and depending on the distance between transmitter and receiver and the altitudes of each. The decision model will attempt to maximize total coverage area for the selection of the optimal

deployment strategy. Ground coverage performance over a large geographic area increases non-linearly as tolerable path loss and aircraft altitude increases. This is due to irregular terrain, atmospheric losses and free-space propagation between transmitters and receivers. In Chapter 9, coverage area versus cost will be presented to illustrate the marginal benefit of coverage area for increasing cost. The presentation of the marginal benefit of coverage area versus cost can provide stakeholders with an opportunity to articulate what an appropriate amount of coverage area is for a given deployment based on the data shown, which can aide in the down-selection of candidate architectures.

6.3 Site-to-Site Connectivity

Link margin for site-to-site connectivity between aircraft will consist of the same link margin computation as for ground coverage. For each site, link margin will be computed for the candidate radio receiver hosted on Aircraft 1 and on Aircraft 2 to all possible transmitters at each site. For a given receiver, the total number of link margin calculations is 22, one for each aircraft type at each of the 11 sites. Transmitters are placed on both candidate aircraft at the other 11 sites so that the receiver computation for a given aircraft/radio pair will be calculated for both aircraft types at the transmitting site. This computation will also utilize the TIREM path loss model at 1350 MHz. A single computation from a transmitter on an aircraft to a receiver on the candidate aircraft is obtained from Eq. (6).

The antenna gain for a given transmit/receive computation will vary in this computation as well, depending on the look angles imposed by the geometry of the transmit/receive pair. Note that aircraft will be placed at the described altitudes above ground level, and the variable terrain for the region analyzed will impose unique geometries and link margins for each aircraft combination. The decision model will attempt to maximize the average number of point-to-point links for the optimal deployment strategy. As is the case for ground coverage calculations, site-to-site connectivity also displays non-linear degradation due to propagation losses.

7 Enumeration of Trade Space

The measures of performance described above must be enumerated for each of the candidate architectures to evaluate against a multi-objective decision problem that maximizes site-to-site connectivity and ground coverage area while minimizing cost. In order to enumerate these trade spaces, the measures of performance relating to link performance (ground coverage area and site-to-site connectivity) must be computed at each site being considered. These measures must be made for each aircraft/radio combination at each site requiring a total of four possible combinations. Each combination must be evaluated for total ground coverage area and site-to-site connectivity for a total of eight data sets per site. Enumerating these data sets for each aircraft/radio pair individually across all sites facilitates the architectural evaluation by calculating the total architecture performance (coverage area, average number of crosslinks, and cost) in the decision model when searching for the optimal deployment. The enumeration of link metrics is described further below.

7.1 Ground Coverage Computations

STK can be utilized to calculate link margin from a given aircraft/radio pair to a ground vehicle over the large geographical area being analyzed. The ground coverage dataset consists of sampling an area target, which in this analysis, is a 308 km x 195 km region that encompasses the geographic region that could be covered by Radio A or Radio B on the aircraft located at the deployment sites. This area target must be large enough to capture all potential points that could have link margins above 0 dB and must be large enough to evaluate ground coverage for the candidate architecture that has the largest ground coverage (in terms of area covered). The "best" architecture for ground coverage is provided by hosting Radio B on Aircraft 2 at all 12 sites. This architecture will provide the best ground coverage performance because Radio B offers better range performance over Radio A due to the higher tolerable path loss. In addition, Aircraft 2 loiters at a higher altitude and provides the greatest LOS footprint to ground vehicles. The area target is held constant for all ground coverage computations to ensure that each grid point for which the link margin is computed is constant for all coverage computations.

The coverage computation for each aircraft/radio pair uses a grid point spacing of 3 km to down-sample the large geographic area being analyzed, resulting in 8400 total grid points. This grid of points results in each point representing coverage for a 7.22 km^2 area. A depiction of this grid spacing is shown in Figure 9 below with each green point representing a position for which a link margin computation will be made. The ground vehicle equipped with the candidate radio will be placed at each point for a given aircraft/radio pair. The data set generated will consist of the link margin to the ground vehicle at each latitude and longitude for which a green point is located for each aircraft/radio pair.

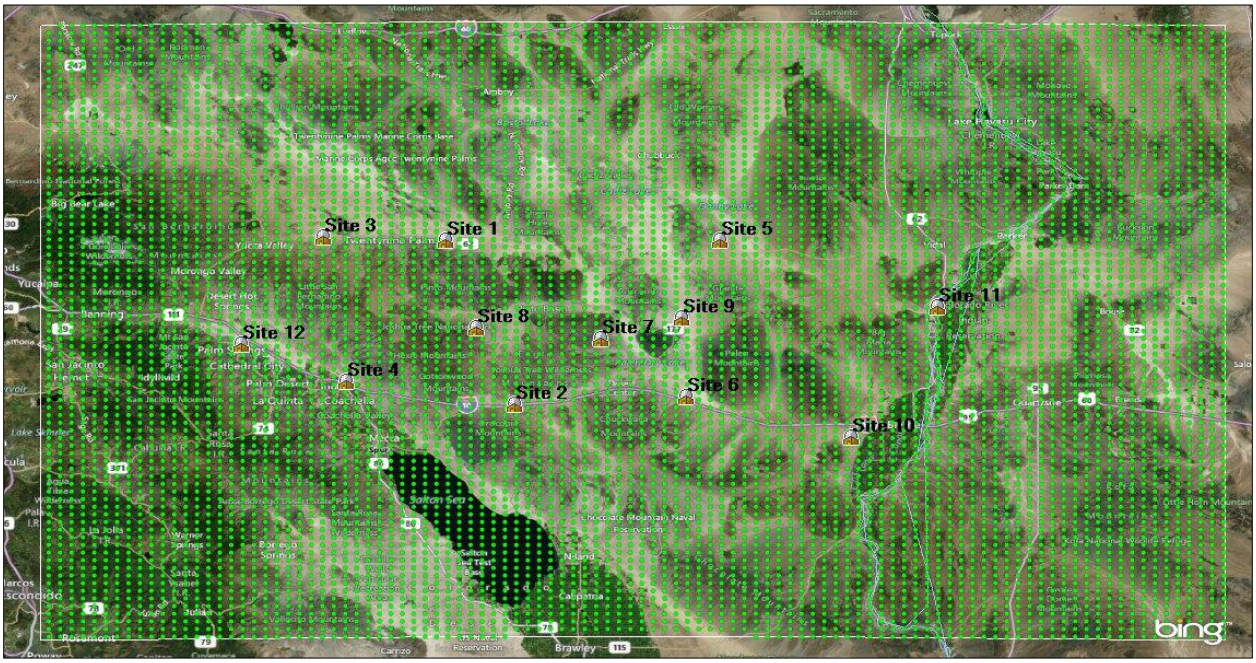

Figure 9. Ground Coverage Computation

The report data generated consists of a matrix of link margin computations and the latitude and longitudes corresponding to the grid point. Note that the ground vehicle antenna is placed at a height of 10 feet above the local terrain altitude (relative to mean sea level) for this computation. Using the local terrain altitude will ensure grid points are placed based on the irregular terrain throughout the region so these local terrain effects can be accounted for in the path loss computation. A sample of this data is shown in Table 10 below highlight a subset of the grid points and corresponding figures of merit (link margin).

Table 10. Sample Data for Ground Coverage Computation for Aircraft/Radio Pair

Latitude (deg)	Longitude (deg)	Link Margin (dB)
34.126	243.22	0.0
34.126	243.295	0.0
34.126	243.371	2.1
34.126	243.447	0.0
34.126	243.523	4.2
34.126	243.598	0.0
34.126	243.674	3.3
34.126	243.75	0.0
34.126	243.826	10.7
34.126	243.902	13.5
34.126	243.977	17.7
34.126	244.053	26.1
34.126	244.129	28.3
34.126	244.205	18.6

7.2 Site-to-Site Connectivity

Site-to-site connectivity must be enumerated for each aircraft/radio pair at each site, requiring four computations per site. Data for each radio set can be consolidated into a single matrix of link margins at each site for a candidate radio. The enumeration of all site accesses can be automated in STK through a script that generates each access computation across all possible aircraft pairs. A sample excerpt from the Radio B connectivity matrix is shown below with each entry representing the link margin in dB. For this particular subset of data, the matrix is indicating that if Aircraft 2 was located at Site 2, it would have a link margin of 11 dB from Aircraft 2 located at Site 12. From this matrix, average number of crosslinks can be calculated computationally for a given candidate architecture.

Table 11. Sample Radio B Site-to-Site Connectivity Matrix

		Site 1		Site 2				Site 12	
		Aircraft 1 Link Margin (dB)	Aircraft 2 Link Margin (dB)	Aircraft 1 Link Margin (dB)	Aircraft 2 Link Margin (dB)	…	…	Aircraft 1 Link Margin (dB)	Aircraft 2 Link Margin (dB)
Site 1	Aircraft 1 Link Margin (dB)	0	0	0	0	…	…	0	0
	Aircraft 2 Link Margin (dB)	0	0	0	0	…	…	0	0
Site 2	Aircraft 1 Link Margin (dB)	0	0	0	0	…	…	0	0
	Aircraft 2 Link Margin (dB)	0	0	0	0	…	…	0	11
	…	…	…	…	…	…	…	…	…
	…	…	…	…	…	…	…	…	…
Site 12	Aircraft 1 Link Margin (dB)	0	0	0	11	…	…	0	0
	Aircraft 2 Link Margin (dB)	0	0	0	0	…	…	0	0

8 Multi-Objective Optimization Model

To perform the architecture evaluation, a multi-objective optimization (MOO) model is implemented to inform the decision of selecting an optimal architecture. In a MOO problem, there is no global optimum that can be selected, but rather a set of solutions that satisfy the Pareto optimal criteria [2]. A mathematical definition of Pareto optimality is presented in 8.1 and can be described as the set of non-dominated solutions that minimizes one objective function that cannot be minimized further without making the other objective functions worse [3].

Marler and Arora describe algorithms that can be utilized by system architects for evaluations in which there is no articulation of preferences by stakeholders [2]. Genetic algorithms are presented for finding nearly global optimums in MOO decision problems to yield a Pareto front and will be applied for the MOO model presented in subsequent sections. In the absence of preferences in performance metrics by stakeholders, a Pareto front can be advantageous to decision-makers by presenting a range of options for candidate architecture. The Pareto front consists of the set of solutions that satisfy the Pareto optimality criteria, which in this case are cost, coverage area and site-to-site connectivity. The articulation of preferences after the Pareto front is determined is beneficial because the articulation of preferences prior to knowing the respective costs and benefits of candidate architectures is both difficult and subjective. The difficulty arises from the uncertainty presented in a large number of candidate architectures and an absence of data highlighting the benefits of candidates. In this particular analysis of aerial layer communications architectures, a priority of the measures of performance to optimize is not realistic, as the goals of such a system are simply to maximize link coverage and connectivity while minimizing cost. Attempting to quantify these preferences is not practical for evaluating the optimal system architectures. Therefore, the Pareto front can be utilized as the set of architecture options that system designers can choose from and to make the understanding of tradeoffs among these options feasible.

No equality constraints are placed on the MOO problem, as they are not needed for this evaluation. The possibility exists that system architects designing a communications architecture in this application would require certain sites to receive communications assets based on mission needs, but these constraints are not imposed for this analysis. The MOO model attempts to highlight the incremental benefits of deploying aircraft/radio pairs to an increasing number of sites, so limiting evaluation of sites through equality constraints will prohibit this insight. The decision consists primarily of assigning a binary 0 or 1 to each aircraft type at a given site such that only one aircraft is selected for a given site, and two aircraft deployed to the same site is not considered practically feasible. This imposes an inequality constraint on the architecture such that the sum of aircraft at a given site must be less than or equal to 1.

8.1 Definitions

Marler and Arora present a definition of Pareto optimality in [2] which is described below. Additional terminology and definitions introduced below are consistent with the definitions provided in [2], with additional definition as the terms relate to this analysis.

x: the design variables in the MOO model consisting of a binary 0 or 1 for each aircraft type at a given site. The size of this vector is 24 (twice the number of sites) where odd indices indicate the number of Aircraft 1 at a given site (0 or 1), and even indices indicate the number of Aircraft 2 at a given site (0 or 1).

F(**x**): this is the vector of objective functions that map the design variables to the three measures of performance (ground coverage area, site-to-site connectivity and cost).

F_1(**x**): the objective function which computes the total cost for the architecture specified by the decision variables in **x**.

F_2(**x**): the objective function which computes the total ground coverage for a given architecture specified by **x**. While the intent of the MOO decision model is to maximize this measure of performance, the formulation of the objective function must be specified as a minimization problem, so total coverage area for a given architecture computation will be returned as the additive inverse of total coverage area computed.

$F_3(\mathbf{x})$: the objective function which computes the average number of site-to-site links for the architecture specified by **x**. This objective must also be formulated as a minimization problem, so the objective function computation will return the additive inverse of the average number of site-to-site links.

$g_j(\mathbf{x})$: the inequality constraints placed on the architectures specified by **x**. Note that this constraint function will impose pair-wise constraints on the use of Aircraft 1 and Aircraft 2 at a given site, such that the sum of Aircraft 1 and Aircraft 2 at a given site must be less than or equal to 1.

Pareto Optimal: A point, $\mathbf{x}^* \in \mathbf{X}$*, is Pareto optimal iff there does not exist another point,* $\mathbf{x} \in \mathbf{X}$, *such that* $\mathbf{F}(\mathbf{x}) \leq \mathbf{F}(\mathbf{x}^*)$*, and* $F_i(\mathbf{x}) < F_i(\mathbf{x}^*)$ *for at least one function.* [2]

8.1.1 Multi-Objective Optimization Problem Definition

The MOO problem is defined below based on the definition in [2] such that the vector of objective functions will be minimized for the decision vector of design variables in **x**:

$$\underset{x}{\text{Minimize}}\ \mathbf{F}(\mathbf{x}) = [F_1(\mathbf{x}), F_2(\mathbf{x}), F_3(\mathbf{x})] \tag{8}$$

$$\text{subject to } g_j(\mathbf{x}) \leq 0 \qquad j = 1,2\ldots,24$$

The MOO model will return all architectures **x** that lie on the Pareto front and the corresponding objective function values. From this Pareto front, an analysis of the optimal architecture can be conducted to select the architecture to deploy.

8.2 Objective Function Description

The objective functions are presented below using pseudocode which is the basis for each function to be implemented in software through the use of MATLAB. The MATLAB implementation is discussed in 8.4 and details the MOO algorithms utilized to generate the Pareto front.

8.2.1 Cost Objective Function

Pseudocode for the cost function, $F_1(\mathbf{x})$, is shown below. This function consists of returning the total cost for a given architecture. Because **x** is arranged such that odd indices map to Aircraft 1 and even indices map to Aircraft 2, the function must check for a binary 1 in each index to determine the total of each aircraft type. The cost computation consists of calculating the cost of the candidate radio on the given aircraft deployment.

```
for i = 1 to length(x)
   if i is odd and x(i)  = 1
      Aircraft 1 Total = Aircraft 1 Total + 1
   else
   if i is even and x(i) = 1
      Aircraft 2 Total = Aircraft 2 Total + 1
   end
end
F1(1) = Aircraft 1 Total * (Aircraft 1 Cost + Radio Cost) +
            Aircraft 2 Total * (Aircraft 2 Cost + Radio Cost)
Return F1(x)
```

8.2.2 Ground Coverage Objective Function

The objective function for calculating ground coverage, $F_2(\mathbf{x})$, takes as its inputs the decision vector **x** and the ground coverage matrix for all aircraft types for the 12 site deployment. The matrix contains link margin computations to the ground vehicle at the latitudes and longitudes of the grid points described in 7.2 for a total of 8400 grid points. The resulting matrix is of size 8400 x 24 and contains the link margins as the elements. This matrix must be parsed for the given deployment specified by **x** and will contain multiple link margin values exceeding 0 dB at a given grid point. The objective function determines the maximum link margin at a given grid point where x_i is equal to 1 and determines the number of unique points in the area target that have a maximum link margin greater than 0 dB, indicating successful closure of the radio link

from an aircraft to a ground vehicle. The combining of ground coverage by picking the maximum link margin at a given point from all sites imposes additional non-linearity beyond those presented in the ground coverage computation. Picking the maximum link margin at a given point is appropriate because it will indicated the highest performance link from all of the aircraft in the current architecture to a ground vehicle. The number of grid points exhibiting non-zero link margins is multiplied by the area of a single grid point, which is 7.22 km^2. This grid size is determined by the geographic area targeted and the grid spacing.

```
for i = 1 to number of grid points
   Grid Point Data Vector = x .* Link Margin Vector(i);
   Max Link Margin = max(Grid Point Data Vector)
   if Max Link Margin > 0
      Total Covered Points  = Total Covered Points + 1;
end
F2(x) = -1*(Total Covered Points)*7.22;
Return F2(x)
```

8.2.3 Site-to-Site Connectivity Objective Function

The site-to-site connectivity objective function, $F_3(\mathbf{x})$, takes the decision vector **x** and a matrix of link margins for all aircraft combinations at the 12 sites. The enumeration of this data set is described in 7.2 and consists of a 24 x 24 matrix where a given row has as its elements the link margins to a given aircraft type at a given site. The first row of this matrix represents the link margins from all sites using either Aircraft 1 or Aircraft 2 to Aircraft 1 at sites where the current architecture decision variables are non-zero to Aircraft 1 at Site 1. Prior to evaluating the row vector at a given site, the Link Margin Matrix and the current architecture decision variables must be multiplied element-by-element. This step ensures that only aircraft being used in the current architecture decision variables are evaluated for connectivity, and not aircraft for which connectivity may exist, but are not utilized in the current iteration. The current architecture is determined by multiplying the 24x1 vector **x** by the transpose of **x**, resulting in a 24x24 matrix.

This function will compute the average number of site-to-site links in the candidate architecture specified by **x** and return the additive inverse.

```
for i = 1 to number of sites
   if x(i) == 0
      continue
   else
      Number of Aircraft = Number of Aircraft + 1
      Current Architecture = x * x^T;
      Site Access Matrix = Current Architecture .* Link Margin Matrix[I,:]
      for j = 1 to number of sites
         if Site Access Matrix(i,j) > 0
            Number of Links = Number of Links +1;
      end
end
F3(x) = -1*(Number of Links/Number of Aircraft in x);
Return F3(x)
```

8.3 Enumeration of the Pareto Front

The enumeration of the Pareto front for the vector of objective functions can be accomplished through the use of a Genetic Algorithm (GA). The Genetic Algorithm is an evolutionary computation technique that relies on principles of natural selection to search for the best solution to a decision problem presented by Holland in 1975 in [8]. GAs can be utilized to search through the entire set of feasible solutions in a MOO decision problem and yield the Pareto front. For decision problems involving objective functions that are non-linear or discontinuous, the Genetic Algorithm is often better-suited than standard optimization algorithms [6]. Because the GA does not require any knowledge beyond what is specified in the objective functions, it can find a global or near-global optimum for discrete and non-linear search spaces such as the MOO problem posed in 8.1.1[6]. The GA can be applied to MOO problems specifically for

generating the Pareto front in order to identify the alternative solutions being sought for this architecture evaluation.

8.3.1 Genetic Algorithm Overview

A simple GA consists of three sequential steps imitating natural selection which are iterated over to traverse the search space utilizing the fitness function. In the context of GA, fitness functions are synonymous with objective functions, and the term fitness function is typically utilized to describe the fitness of given individuals to reproduce offspring in subsequent generations. These steps consist of selection, crossover, and mutation with the goals of these steps to find the fittest "individuals", which in this case are the candidate architectures on the Pareto front [7].

- *Selection*: randomly selects "individuals" (candidate architectures) for reproduction based on probabilities depending in fitness functions which allows for the fittest architectures to be selected with a higher probability. The fitness functions in this case are the objective functions described in 8.2.
- *Crossover:* This step randomly chooses bits in the bit string from two selected individuals to combine into offspring in the subsequent generation of the algorithm execution.
- *Mutation:* Mutation is applied throughout the execution of GA by randomly flipping bits in the bit strings of individuals, typically with some small probability. The intent of this step is to reduce the likelihood of the algorithm getting stuck in a local optimum.

Algorithm Execution

The execution of the steps described above comprising a simple GA is described in [7] as follows:

1. Choose random starting population of n individuals, this is also called the initial population. A "creation function" is employed to select the initial population probabilistically based on the fitness of individuals.
2. Calculate the fitness function for each individual of the population.

3. Repeat the selection, crossover, and mutation steps until a new population of n individuals is created. Each new population is called a “generation”.
    - Select two individuals from the current population with the probability of selection increasing based on the fitness function provided.
    - Combine the two selected individuals randomly to yield two offspring based on some crossover probability.
    - Randomly apply a mutation to bits in the two offspring based on some mutation probability. Note that the mutation of bits in the two offspring occurs at some small probability, and will not occur in most offspring.
4. Replace the current population with the new n offspring generated in step 3.

Steps 2 through 4 are repeated for a set number of iterations or if the improvement in fitness in subsequent generations falls below some threshold improvement. The steps of the simple GA described by Mitchell on a population of candidate architectures are shown in Figure 10. Note that in this application of the GA, intermediate measures of performance were computed offline to be utilized in the architecture evaluation examining cost, coverage area performance and average number of crosslinks as the algorithm executed.

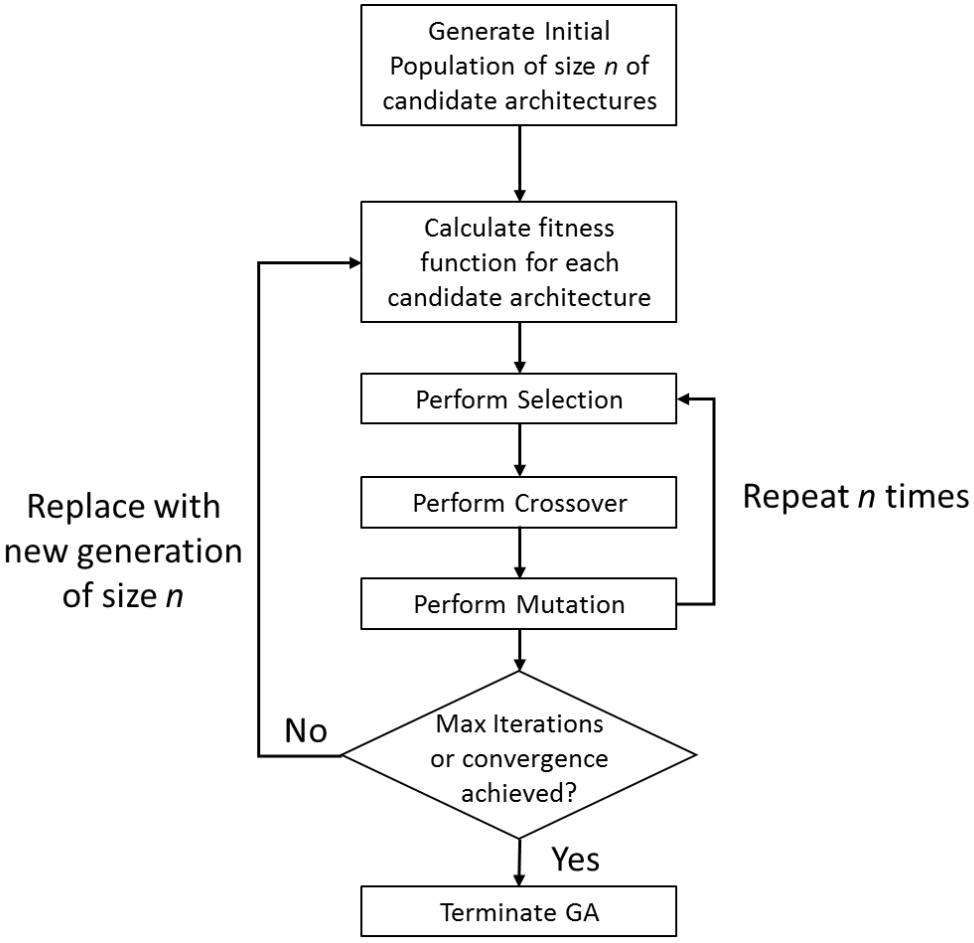

Figure 10. Simple GA Flow Chart

Limitations of Genetic Algorithm

The intent of the GA is to find a solution to an optimization problem by searching a fraction of the entire search space of candidate architectures, which can be very large. The output of the GA is a candidate architecture that is near-optimal or on the Pareto front, or optimal without examining the entire search space [7]. For the evaluation of the 12 site deployment for a communication system architecture, GA is an appropriate method because the number of architectures is quite large and can grow further with the addition of more sites beyond the 12 considered in this analysis. The lack of a complete evaluation of the search space can lead to solutions that are not truly optimal and the potential exists for premature termination if the maximum number of iterations is reached. Additionally, convergence criteria based on incremental improvements in the fitness function that fall below the required threshold can

lead to premature termination [6]. However, given the large number of permutations for candidate architectures, near-optimal solutions will suffice for this architecture evaluation.

8.4 MATLAB Decision Model Implementation

The MATLAB computing environment is utilized to implement the objective functions described in 8.2 as well as the enumeration of the Pareto front using the multi-objective GA. MATLAB was selected as the appropriate tool for implementing the MOO decision model because of the availability of a multi-objective GA implementing in the Global Optimization Toolbox and the capabilities of MATLAB to perform data analysis on the Pareto front returned from execution of the multi-objective GA. In addition, MATLAB is widely used for numerical computing and data analysis applications in engineering organizations and is readily available for student use.

8.4.1 MATLAB Global Optimization Toolbox

The MATLAB Global Optimization Toolbox is a MATLAB add-on providing functions to perform optimization and searches for global solutions that contain multiple maxima or minima [10]. Additionally, it provides a customizable GA function that allows users to tailor the GA based on initial populations or different crossover, selection and mutation functions. For this analysis, the gamultiobj solver is utilized to enumerate the Pareto front of the three objective functions. The implementation of the gamultiobj solver is based on the non-dominated
sorting genetic algorithm II (NSGA-II) presented in [9].

gamultiobj Solver Settings

The gamultiobj solver attempts to return the Pareto front for the objective functions and corresponding decision variables specified in the function call. As discussed, the decision variables consist of the 24-element vector, **x**, indicating the aircraft type chosen at each site. Because these decision variables are binary, the gamultiobj solver must be configured to operate on a bit string population. The population utilized in gamultiobj and the decision variables are synonymous. In the current implementation of gamultiobj, all constraints are ignored when operating on populations of type bit string [11]. To address the inability to

express constraints, the MOO model applies severe penalties to infeasible architectures to prevent these architectures from appearing on the Pareto front.

Initial Population Settings

Initial populations can be specified prior to running gamultiobj where a user can specify a candidate architecture that is believed to be advantageous with respect to one or more objective functions to speed up convergence of the algorithm. In this application, there is no prior knowledge or articulation of what an advantageous architecture is, therefore the default settings are used. The default initial population is generated randomly at the start of gamultiobj. A sensitivity analysis is presented in 9.3 which examines gamultiobj outputs for two different initial populations.

Constraint Settings

As stated above, constraints are ignored for population types that are bit strings. In the MOO problem definition in 8.1.1, a constraint was placed on the candidate architectures that only one instance of a type of aircraft can be selected at a given site. This constraint is intended to prevent the use of two different aircraft types at a given site, however gamultiobj does not allow this constraint to be applied.

Two approaches were considered to address the possibility of Aircraft 1 and Aircraft 2 being deployed at a single site and being on the Pareto Front. The first approach consists of simply throwing out these architectures from the Pareto front after gamultiobj terminates. The second approach consists of checking for this condition in the objective functions and simply returning a high cost and poor link performance for this architecture. This has the effect of removing architectures that pick multiple aircraft at a given site from the Pareto front. The first approach was attempted for this architecture evaluation because it is easy to throw out such points after the Pareto front is enumerated, and allows designers to at least consider the costs and benefits of such a deployment. However, this approach yielded too many points on the Pareto front containing multiple aircraft at a single site. Furthermore, the prevalence of these architectures

on the Pareto front could indicate that the gamultiobj function returned architectures that were non-dominated on the dimension of cost, coverage area or average number of crosslinks. While pairwise evaluation of aircraft counts at each site does not scale well as the number of sites increases, this approach was utilized and documented in Appendix A. Evaluation of the Pareto front after the termination of gamultiobj indicated that no sites on the Pareto front included multiple aircraft at a given site.

9 Architecture Evaluation Results

The Pareto front was generated for Radio A and Radio B separately using the MOO decision model described above. Results for each radio type are presented together with the intent of down-selecting from the Pareto front for each radio type to select to optimal architectures for each radio system. From these selected architectures, an analysis of the respective performance of each radio type is presented.

9.1 Performance Results

In order to evaluate the performance of Pareto optimal architectures, the Pareto front can be analyzed for each pair-wise combination of fitness functions. While the Pareto front returned by the MOO model returns the non-dominated Pareto front in the three dimensions analyzed, the Pareto front is presented in two dimensional space for the three combinations. The figures below plot performance of total coverage area vs. cost, average site-to-site connectivity vs. cost, and average site-to-site connectivity vs. total coverage area. From these pair-wise comparisons of performance, heuristics can be applied by system architects to further down-select from the Pareto front to a handful of candidate architectures for more detailed analysis. For each radio type, the total population of architectures generated by gamultiobj was approximately 350 architectures. For Radio A, the Pareto front consisted of 54 architectures, while the Pareto front for Radio B consisted of 49 architectures.

9.1.1 Total Coverage Area vs. Cost

Coverage area vs. cost is presented in Figure 11. From this plot, coverage performance for both radio systems levels off at around a cost of $80 million from which there is only a small incremental improvement in coverage performance for larger improvements in cost. This data suggests that coverage area in the $60-$80 million range is worth evaluating in more detail against the site-to-site connectivity performance. In this comparison of fitness functions, a clear indication of the leveling off of performance can aid system architects in down-selecting to a subset of Pareto optimal candidate architectures. This figure also highlights the significant

performance advantage offered by Radio B based on the higher tolerable path loss from airborne assets to a ground vehicle.

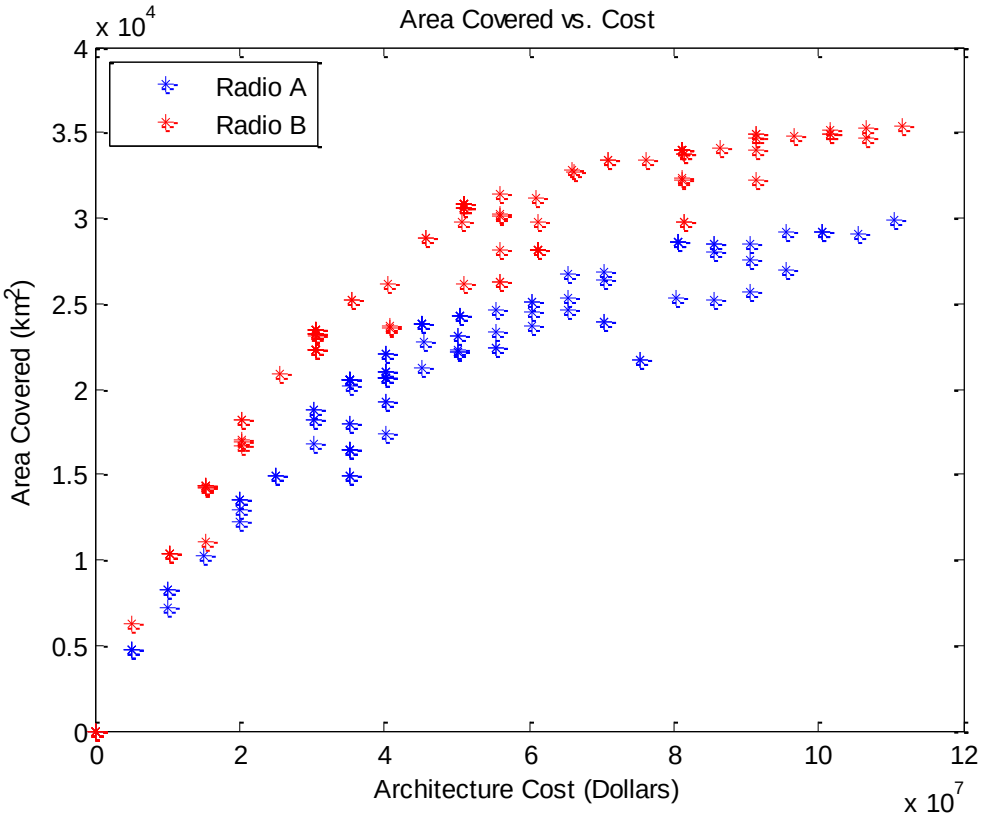

Figure 11. Area Covered vs. Cost

9.1.2 Site-to-Site Connectivity vs. Cost

A comparison of site-to-site connectivity vs. cost is presented in Figure 12. For both radio types, there is a leveling off in the peak average number of crosslinks per site as the architecture cost increases. However, the spread in performance for the average number of crosslinks versus cost in the Pareto front makes focusing on a subset of architectures difficult. If this Pareto front is pared using the architectures in the $60 - $80 million range gleaned from Figure 11, an evaluation of the network topologies of this subset of Pareto optimal architectures can be conducted. While the average number of crosslinks metric is useful for yielding a Pareto front based on high-level needs, additional analysis is required to gain more insight into the differences in network performance for the remaining architectures in the $60 - $80 million range.

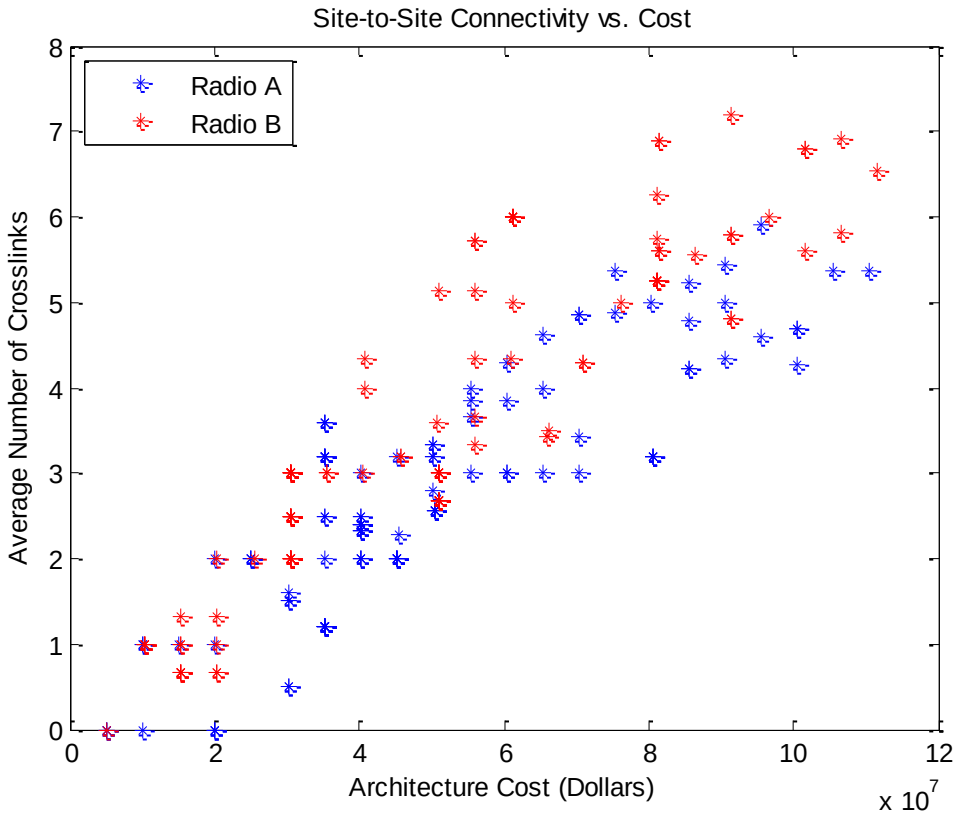

Figure 12. Average Number of Crosslinks vs. Cost

9.1.3 Site-to-Site Connectivity vs Area Covered

Site-to-Site connectivity vs. area covered for each radio type is shown in Figure 13. Similar to the comparison presented in 9.1.2, a clear leveling off of site-to-site connectivity versus area covered is not apparent. However, for Radio A there is a cluster of Pareto optimal architectures in the 24,000 to 30,000 km^2 region of total area covered. Similarly, there is clustering in architectures utilizing Radio B in the 28,000 – 35,000 km^2 region of total area covered. Down-selecting from the Pareto front to architectures in these regions can potentially reveal a small subset of optimal architectures when combined with the cost sensitivities presented in 9.1.1, where architectures in the area of $60 - $80 million provide the best balance of coverage area and cost. While this performance comparison does not clearly inform a down-selection of candidate architectures, it can be utilized to infer "good" architectures requiring more detailed analysis in the network topologies.

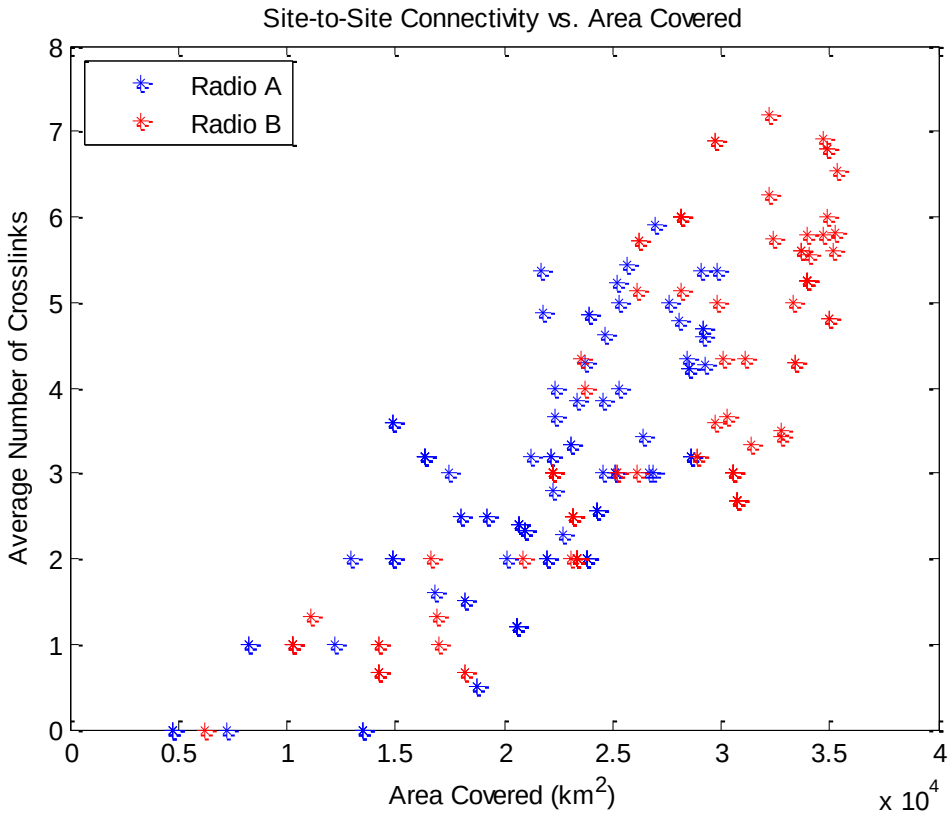

Figure 13. Average Number of Crosslinks vs. Area Covered

9.2 Down-Selection from the Pareto Front

From the Pareto fronts presented above, candidate architectures in the range of approximately $60 - $80 million will be considered to further evaluate site-to-site connectivity. Figure 11 indicates a leveling off of coverage area performance versus cost and can be used as a basis for down-selecting from the Pareto front for evaluating the network performance embodied in the Site-to-Site connectivity matrix. For the purposes of this analysis, an assumption is made that this range of total cost is acceptable to decision makers. Evaluating the best topologies from this subset is made more manageable by only considering the architectures where the coverage area vs. cost comparison yields the best value.

9.2.1 Radio A Down-Selection of the Pareto Front

After filtering the Pareto front to the range of acceptable costs described above, the remaining Pareto front is reduced to 13 candidate architectures from the original 54. The down-selected Pareto front is summarized in Table 12.

Table 12. Down-Selected Pareto Front for Radio A

Site	1		2		3		4		5		6		7		8		9		10		11		12		Cost	Area (km^2)	Average Crosslinks	# of Sites
Platform	1	2	1	2	1	2	1	2	1	2	1	2	1	2	1	2	1	2	1	2	1	2	1	2				
Arch 1	0	1	0	1	0	0	0	0	0	1	0	0	0	1	0	0	0	0	0	1	0	1	0	0	$60,300,000	25140	3.0	6
Arch 2	0	1	0	1	0	0	0	0	0	1	0	0	1	0	0	0	0	1	1	0	0	1	0	0	$60,350,000	24548	3.9	7
Arch 3	1	0	0	1	0	0	0	0	0	1	0	0	0	1	0	0	0	1	1	0	0	1	0	0	$60,350,000	23696	4.3	7
Arch 4	0	0	0	1	0	1	0	0	0	1	0	0	0	1	0	0	0	1	1	0	0	1	0	0	$65,350,000	25277	4.0	7
Arch 5	0	1	0	1	0	0	0	0	0	1	1	0	1	0	0	0	0	1	1	0	0	1	0	0	$65,400,000	24642	4.6	8
Arch 6	0	1	0	1	1	0	1	0	0	1	0	1	0	0	0	0	0	0	1	0	0	1	0	0	$65,400,000	26707	3.0	8
Arch 7	0	1	0	1	0	0	0	0	0	1	0	1	0	1	0	0	0	1	0	0	0	1	0	0	$70,350,000	23913	4.9	7
Arch 8	0	1	0	1	0	1	0	0	0	1	0	1	0	0	0	0	0	0	0	1	0	1	0	0	$70,350,000	26432	3.4	7
Arch 9	0	1	0	1	0	0	0	0	0	1	0	0	0	1	0	0	1	0	1	0	0	1	0	1	$70,400,000	26830	3.0	8
Arch 10	1	0	0	0	0	0	0	0	0	1	0	1	0	1	0	1	0	1	0	1	0	1	0	0	$75,400,000	21660	5.4	8
Arch 11	0	0	0	1	0	1	0	0	0	1	0	1	0	1	0	1	0	1	1	0	0	0	0	0	$75,400,000	21754	4.9	8
Arch 12	0	1	0	1	0	1	0	0	0	1	0	1	0	1	0	0	0	1	0	0	0	1	0	0	$80,400,000	25292	5.0	8
Arch 13	1	0	0	1	0	1	1	0	0	1	0	0	0	0	1	0	0	1	0	1	0	1	1	0	$80,500,000	28635	3.2	10

A consolidated summary of Radio A candidate architectures is presented in Table 13, with the addition of total number of sites for the given deployment and the composition of aircraft for a given architecture.

Table 13. Radio A Consolidated Architecture Summary

Architecture	Cost	Area (km^2)	Average Crosslinks	Number of Sites	Number of Aircraft 1	Number of Aircraft 2
Arch 1	$60,300,000	25140	3.0	6	0	6
Arch 2	$60,350,000	24548	3.9	7	2	5
Arch 3	$60,350,000	23696	4.3	7	2	5
Arch 4	$65,350,000	25277	4.0	7	1	6
Arch 7	$70,350,000	23913	4.9	7	0	7
Arch 8	$70,350,000	26432	3.4	7	0	7
Arch 5	$65,400,000	24642	4.6	8	3	5
Arch 6	$65,400,000	26707	3.0	8	3	5
Arch 9	$70,400,000	26830	3.0	8	2	6
Arch 10	$75,400,000	21660	5.4	8	1	7
Arch 11	$75,400,000	21754	4.9	8	1	7
Arch 12	$80,400,000	25292	5.0	8	0	8
Arch 13	$80,500,000	28635	3.2	10	4	6

A bar graph of aircraft composition is provided in Figure 14 and reveals a clear dominance of Aircraft 2 in the remaining candidate architectures, with four architectures consisting of only Aircraft 2. The MOO model only accounted for aircraft cost when generating the Pareto front,

however this data is insightful in that it could aid decision-makers in evaluating the utility of considering both aircraft for deployment. The possibility exists that procuring only one aircraft type could yield cost savings on the procurement cost by purchasing a larger number. Furthermore, the lifecycle costs and logistics footprint could be reduced through the use of only a single aircraft type. Clearly, these cost-savings depend on the individual aircraft themselves, which as defined, are not well understood enough to the make such an assessment in this analysis.

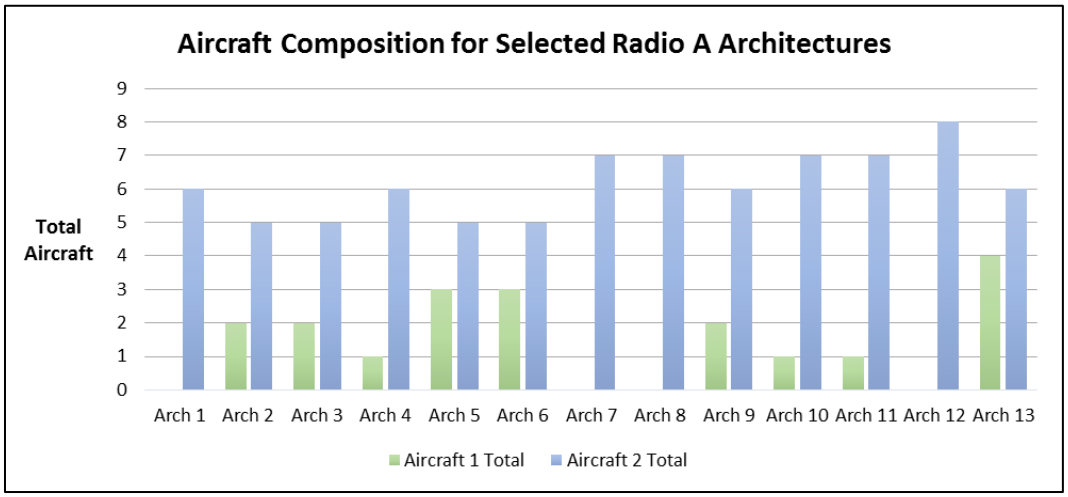

Figure 14. Aircraft Composition for Down-Selected Pareto Front Using Radio A

9.2.2 Radio B Down-Selection of the Pareto Front

Down-selecting from the Pareto front for Radio B on the basis of cost reduces the candidate architectures from 49 to 12. The total coverage area for these candidates is tightly grouped in the 28,000 to 35,000 km^2 region of performance prohibiting further down-selection of the Pareto front on the basis of coverage area. The remaining candidates are summarized in Table 14.

Table 14. Down-Selected Pareto Front for Radio B

Architecture	1		2		3		4		5		6		7		8		9		10		11		12		Cost	Area (km^2)	Average Crosslinks	# of Sites
	1	2	1	2	1	2	1	2	1	2	1	2	1	2	1	2	1	2	1	2	1	2	1	2				
Arch 1	0	1	0	1	0	1	0	0	0	1	0	0	0	0	0	0	0	0	0	1	0	1	0	0	$60,900,000	31140	4.3	6
Arch 2	0	0	0	1	0	0	0	0	0	1	1	0	1	0	0	1	1	0	1	0	0	1	0	0	$61,200,000	28187	6.0	8
Arch 3	0	0	0	1	0	1	0	0	0	1	1	0	1	0	0	0	1	0	1	0	0	1	0	0	$61,200,000	29783	5.0	8
Arch 4	0	0	0	1	0	1	0	0	0	1	0	0	0	0	0	1	0	0	1	0	0	1	0	1	$66,050,000	32757	3.4	7
Arch 5	0	0	0	1	0	1	1	0	0	1	0	0	0	0	1	0	1	0	0	1	0	1	0	0	$66,200,000	32735	3.5	8
Arch 6	0	0	0	1	0	1	0	0	0	1	0	0	0	1	0	0	0	0	0	1	0	1	0	1	$71,050,000	33414	4.3	7
Arch 7	0	0	0	1	0	1	0	0	0	1	0	0	0	1	0	0	0	1	0	1	0	1	1	0	$76,200,000	33335	5.0	8
Arch 8	0	0	0	1	0	1	0	0	0	1	0	0	0	1	0	0	0	1	0	1	0	1	0	1	$81,200,000	33920	5.3	8
Arch 9	0	1	0	1	0	1	0	0	0	1	0	1	0	1	0	0	0	0	0	1	0	1	0	0	$81,200,000	32230	6.3	8
Arch 10	0	1	0	1	0	1	0	0	0	1	0	1	0	0	0	1	0	0	0	1	0	1	0	0	$81,200,000	32367	5.8	8
Arch 11	1	0	0	1	0	0	0	0	0	1	0	1	0	1	0	1	0	1	1	0	0	1	0	0	$81,350,000	29761	6.9	9
Arch 12	0	0	0	1	0	1	0	0	0	1	1	0	1	0	0	1	1	0	0	1	0	1	1	0	$81,500,000	33725	5.6	10

Applying the same methodology described in 9.2.1, the candidate architectures are broken out by aircraft composition and sorted in increasing order by number of sites comprising the candidate architectures and summarized in Table 15.

Table 15. Radio B Consolidated Architecture Summary

Architecture	Cost	Area (km^2)	Average Crosslinks	Number of Sites	Number of Aircraft 1	Number of Aircraft 2
Arch 1	$60,900,000	31140	4.3	6	0	6
Arch 4	$66,050,000	32757	3.4	7	1	6
Arch 6	$71,050,000	33414	4.3	7	0	7
Arch 2	$61,200,000	28187	6.0	8	4	4
Arch 3	$61,200,000	29783	5.0	8	4	4
Arch 5	$66,200,000	32735	3.5	8	3	5
Arch 7	$76,200,000	33335	5.0	8	1	7
Arch 8	$81,200,000	33920	5.3	8	0	8
Arch 9	$81,200,000	32230	6.3	8	0	8
Arch 10	$81,200,000	32367	5.8	8	0	8
Arch 11	$81,350,000	29761	6.9	9	2	7
Arch 12	$81,500,000	33725	5.6	10	4	6

The aircraft composition for the remaining candidate architectures is shown below in Figure 15. As was observed for the Radio A down-selected Pareto front, a clear dominance of Aircraft 2 in the remaining architectures is evident. Six of the remaining architectures utilize Aircraft 2 only and highlight the need to examine potential cost savings that could be realized through the use of a single aircraft type versus the two considered in the architecture evaluation.

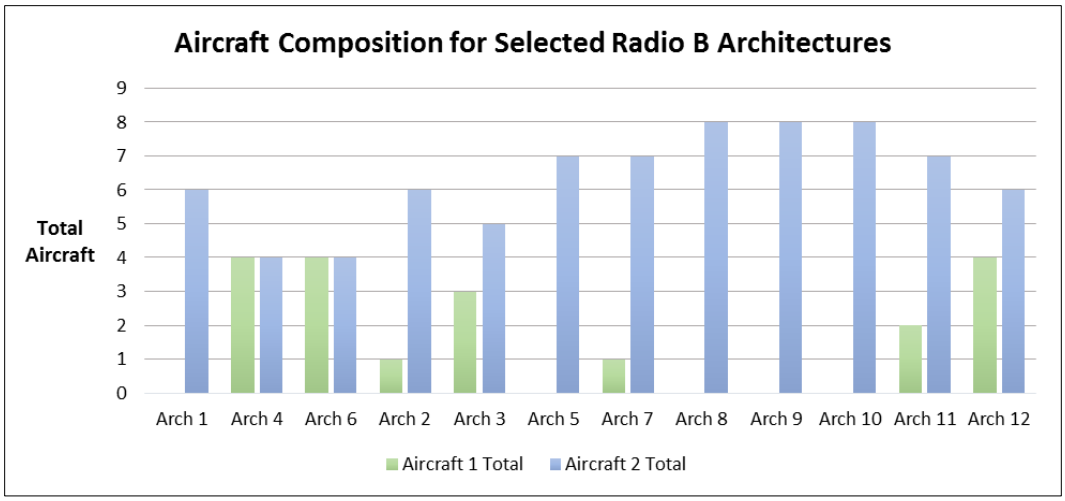

Figure 15. Aircraft Composition for Down-Selected Pareto Front Using Radio B

9.3 Sensitivity Analysis

In order to ensure that the Pareto fronts shown above are adequate for architectural recommendations, a sensitivity analysis can be conducted utilizing different initial populations prior to the execution of gamultiobj in MATLAB. Because gamultiobj does not perform an exhaustive search through all feasible architectures, a sensitivity analysis can provide insight as to whether the Pareto front returned by gamultiobj reflects near-optimal architectures. A comparison can be conducted between the Pareto front enumerated above and two different initial populations. The results presented in this sensitivity analysis focus on Pareto fronts for Radio A returned by using two additional initial populations in order to validate the Pareto front used above. The expectation is that the general trends observed in the Pareto front shown above will be consistent using two different initial populations. The GA implemented in MATLAB returns near-optimal solutions, so the expectation is that while the same near-optimal solutions will not be identical in subsequent runs, the trends should be similar. Because the trends in the Pareto fronts for both Radio A and Radio B are similar, sensitivity analysis on the Radio A Pareto front should provide sufficient validation of the gamultiobj ability to achieve adequate coverage of the search space.

For the first initial population considered, gamultiobj will start with a candidate architecture consisting of the best single site from the perspective of area covered. Deploying Aircraft 2 to Site 11 yields the highest coverage area, so the initial population will be a bit string of zeros, with the exception that a binary "one" will be located in the element corresponding to Aircraft 2 at Site 11. The intent of this initial population is to seed gamultiobj with a solution on the Pareto front.

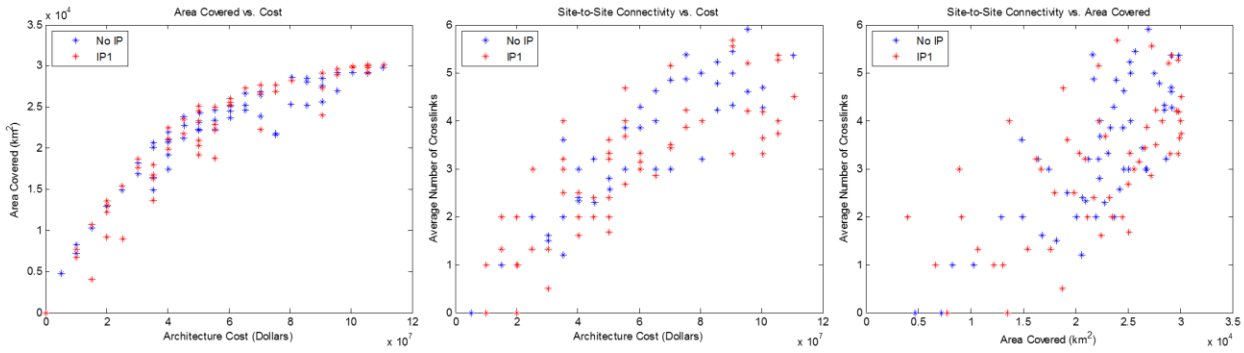

Figure 16. Comparison of Pareto Front to Initial Population 1

The Pareto front shown in Figure 16 for initial population 1 shows comparable performance for area covered versus cost as the Pareto front presented in 9.1. The general trend of average number of crosslinks increasing as cost increases is also observed for initial population 1, though the performance of candidate architectures does not appear to be as strong for Initial population 1 as cost increases. For the comparison of the average number of crosslinks versus area covered, the general trend of initial population 1 matches the original Pareto front, though the performance appears to be more spread out than the baseline Pareto front. There is also a cluster of four points at the upper end of area covered and average number of crosslinks that may warrant exploration as candidate architectures.

The second initial population assumed the "best case" deployment strategy from a performance perspective. This case assumes that architecture cost is de-emphasized and Radio A would be integrated on Aircraft 2 at all sites. This initial population consists of a binary "1" placed at the elements corresponding to Aircraft 2 at all sites, and a binary "0" placed in

elements corresponding to Aircraft 1. The Pareto front for this initial population is shown in Figure 17.

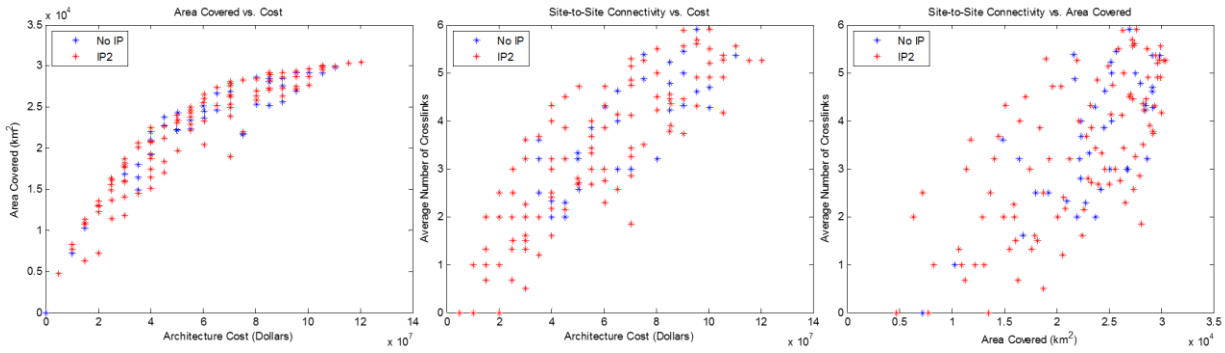

Figure 17. Comparison of Pareto Front to Initial Population 2

The Pareto front using initial population 2 is very similar to the baseline Pareto front when evaluating area covered versus cost. Similarly, the same trends are observed for site-to-site connectivity versus cost are observed, though the spread in Pareto front using initial population 2 is greater, particularly for lower cost architectures. For site-to-site connectivity versus area covered, the trends in the Pareto front both indicate positive correlation for these objectives. Similar to the Pareto front shown for initial population 1, there is a cluster of points for initial population 2 at the upper end of site-to-site connectivity and area covered. These architectures also may warrant further consideration as candidates.

Varying the initial populations for gamultiobj does reveal the potential for some minor differences in the Pareto fronts. The general trends in the Pareto fronts for the various objective functions are consistent though, which increases the confidence level of the baseline Pareto fronts presented in 9.1. However, the varying of initial populations does reveal candidate architectures that could be considered for the architectural evaluation, so a sensitivity analysis consisting of testing at the extremes using initial populations could be useful for further optimizing the MOO model outputs.

10 Detailed Analysis of Selected Architectures

In order to further down-select the candidate architectures, site-to-site connectivity (measured by average number of crosslinks) can be utilized as a metric to further down-select from the Pareto front. Recall that the average number of crosslinks metric is the measure of network performance for candidate architectures to tolerate the loss of individual nodes in the architecture and maximize throughput. For these candidate architectures, understanding the trade off in average crosslinks versus coverage area is necessary, which is illustrated in Figure 18. For Radio A, there is a discernible degradation in average number of crosslinks as coverage area increases. This is likely due to the positions of the sites selected in these candidate architectures. If candidate architectures selected utilize sites that are more geographically spread out, there is a higher likelihood of average number of crosslinks decreasing as more terrain obstructions can limit crosslink connectivity. However, if there is greater spread in the site distances, more unique coverage points are able to be covered in the ground coverage computation. For Radio B, a similar trend is observed where the average number of crosslinks generally decreases as coverage area increases.

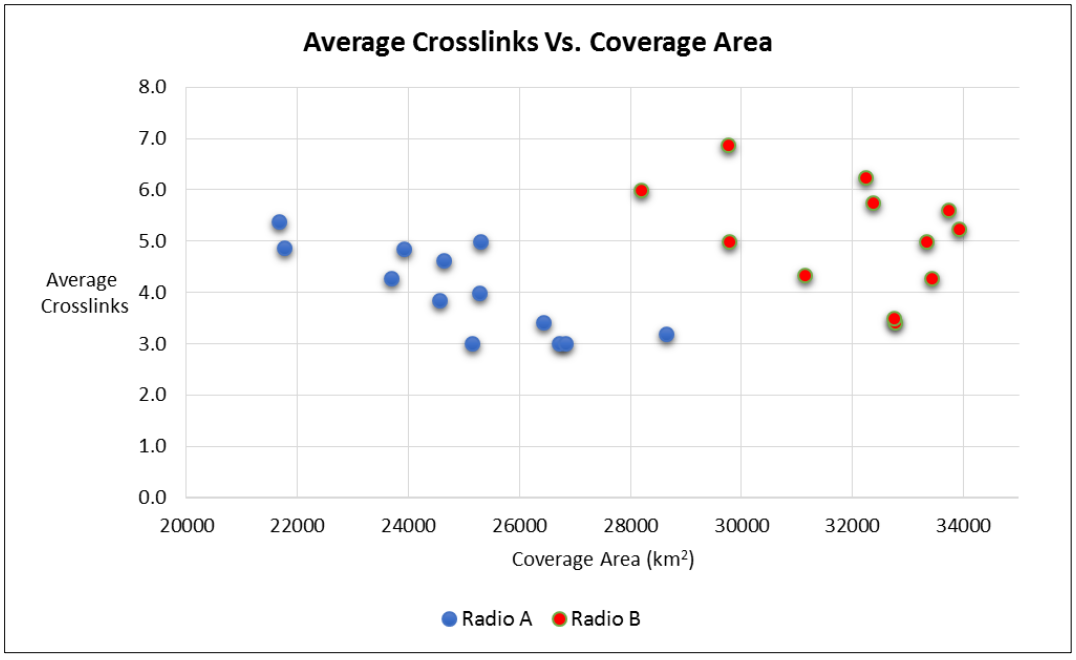

Figure 18. Average Crosslinks vs. Area Covered for Pared Pareto Front

Further down-selecting the candidate architectures from the remaining Pareto front is difficult given the lack of a clear articulation of user needs from stakeholders. The down-selected architectures presented in 9.2 provide a set of candidate architectures that can be utilized by decision-makers to further articulate preferences within this set of architectures. For example, the prioritization of certain sites can be articulated which could remove a subset of the candidate architectures even further. In this analysis, no assumption is made on the relative strength of importance of average number of crosslinks or total area covered. To further down-select the candidate architectures, an assumption is made that three candidates for each type of radio will be selected to conduct a detailed performance analysis to identify the better radio option. To perform this down-selection, it is assumed that the three architectures will consist of the architecture with the highest average number of crosslinks, the architecture with highest total area covered, and the third architecture will consist of an estimate of the midpoint between these two competing requirements. The selected architectures are annotated in Figure 19 below. Note that there the selection of the "midpoint" architecture is subjective in the absence of an articulation of the relative importance of the two metrics analyzed.

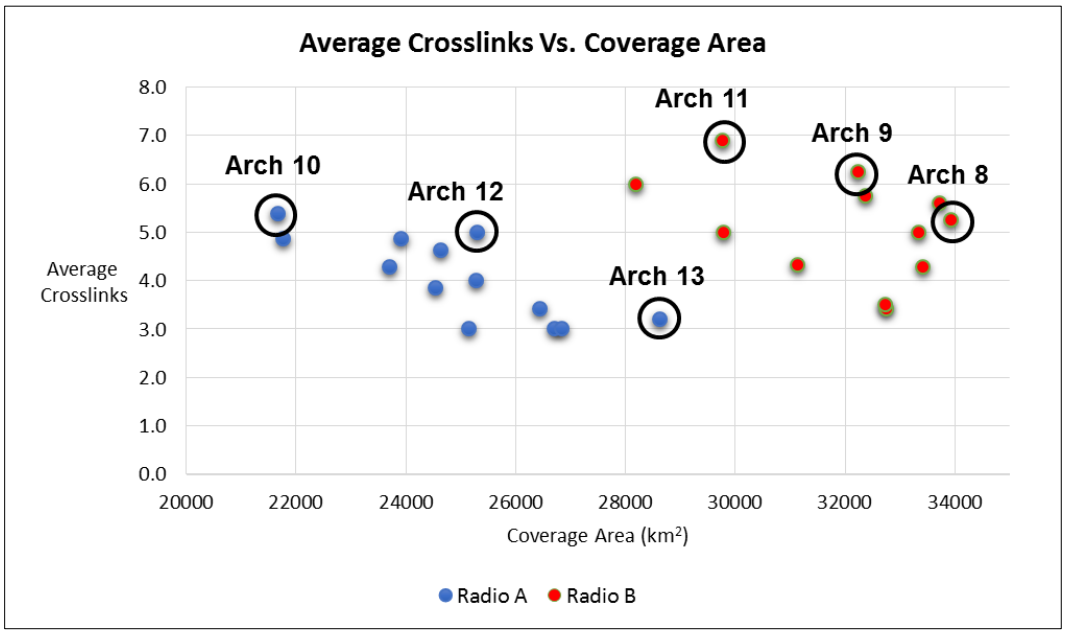

Figure 19. Final Candidate Architectures for Radio A and Radio B

10.1 STK Evaluation of Final Candidate Architectures

The architectures selected for the detailed performance analysis are summarized in Table 16 along with the performance attributes prioritized. The corresponding aircraft and the respective sites in each of the candidate architectures are taken from Table 13 and Table 15. The STK model can be utilized to assess the system-level performance of these candidates for the purpose of comparing performance between Radio A and Radio B. Detailed analysis of the remaining architectures can provide visualization of the architectures to gain insight into the respective benefits and limitations of the remaining architectures. The detailed coverage views are grouped by attribute to facilitate differentiation among the two radios analyzed.

Table 16. Consolidated Final Candidate Architectures

Architecture	Cost	Attribute
Radio A		
Arch 10	$75,400,000	Maximum Site-to-Site Connectivity
Arch 12	$80,400,000	Balance of Site-to-Site Connectivity and Area Covered
Arch 13	$80,500,000	Maximum Area Covered
Radio B		
Arch 8	$81,200,000	Maximum Area Covered
Arch 9	$81,200,000	Balance of Site-to-Site Connectivity and Area Covered
Arch 11	$81,350,000	Maximum Site-to-Site Connectivity

10.1.1 Radio Comparison for Maximum Site-to-Site Connectivity

For the maximum site-to-site connectivity attribute, Radio B appears significantly better both in site-to-site connectivity and area covered. Not only does Radio B possess a denser topology, but the ground coverage area is significantly bigger. Furthermore, the link margins shown throughout the region is predominantly in the blue region (greater than 12 dB). This architecture costs approximately $6 million more than the corresponding Radio A architecture, but offers a significant improvement in performance. Both networks exhibit topologies with

nodes containing multiple links, indicating a degree of tolerance against the loss of a single node and maximal throughput performance.

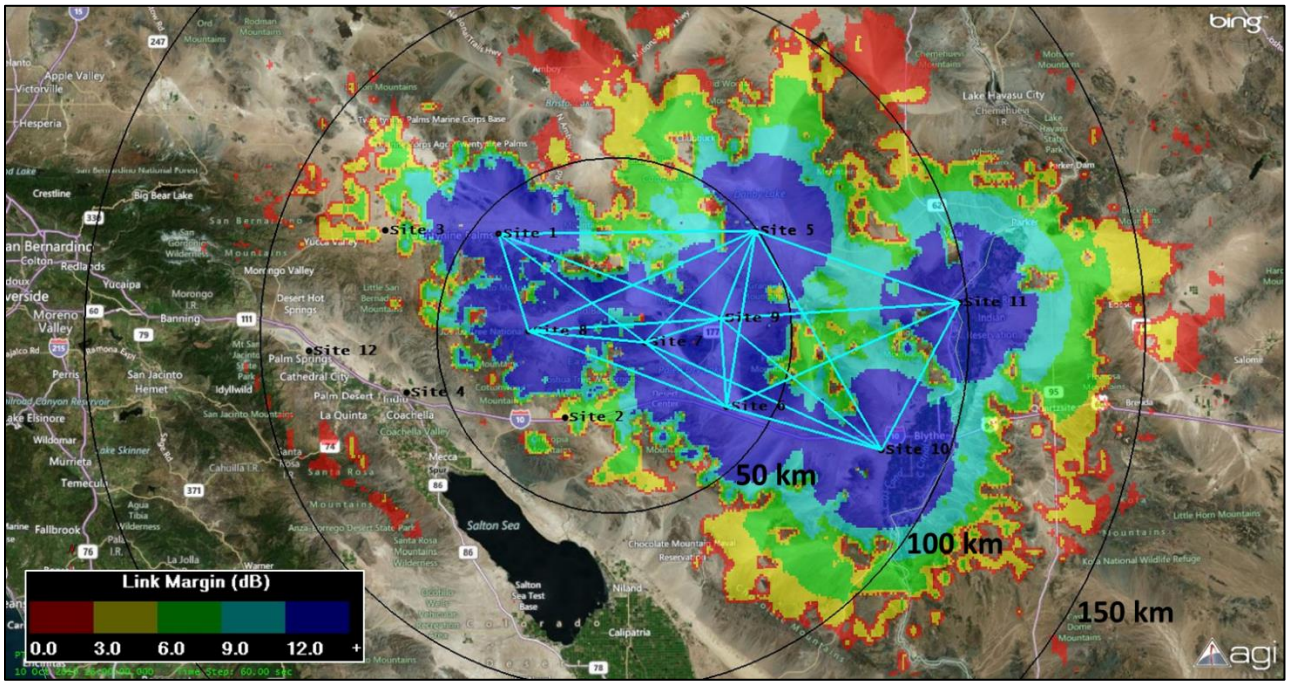

Figure 20. Architecture 10 for Radio A (Maximum Site-to-Site Connectivity)

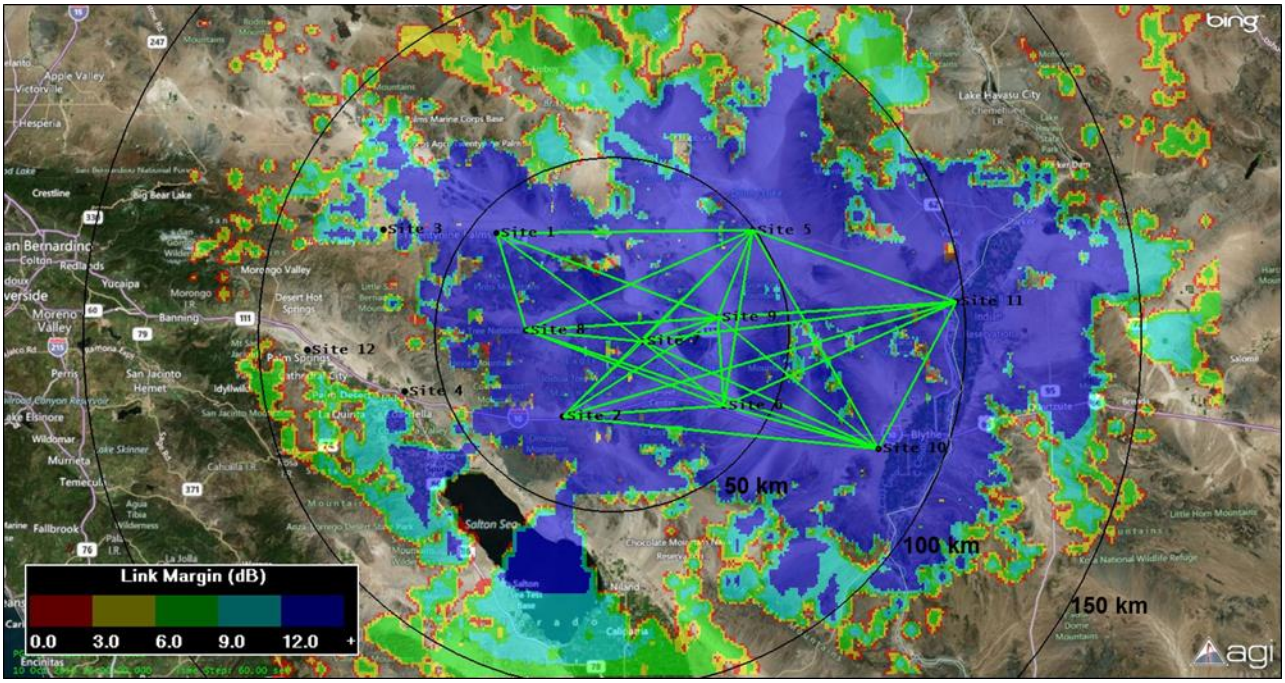

Figure 21. Architecture 11 for Radio B (Maximum Site-to-Site Connectivity)

10.1.2 Radio Comparison for Maximum Area Covered

If total area covered is an attribute prioritized by stakeholders, Figure 22 and Figure 23 illustrate how the inclusion of edge nodes increases the coverage footprint at the cost of average number of crosslinks. This is illustrated at Sites 4 and 12 for the Radio A architecture and at Site 12 for the Radio B architecture. This visualization allows the tradeoff to be made for choosing to deploy to these sites, as stakeholders can weigh the importance of bringing edge nodes into the topology to increase coverage area. However, this topology has fewer point to point links, reducing throughput. These topologies are also less robust to the loss of individual nodes. For example, if the asset at Site 2 cannot operate for a given mission, Sites 4 and 12 will not be able to reach back into the network in the Radio A architecture, and Site 12 would not be able to reach back in the Radio B architecture. As was seen in the previous figures, Radio B appears to offer a significant improvement in performance for both site-to-site connectivity and ground coverage. This architecture costs a fraction more than the corresponding Radio A architecture, costing only $700,000 more.

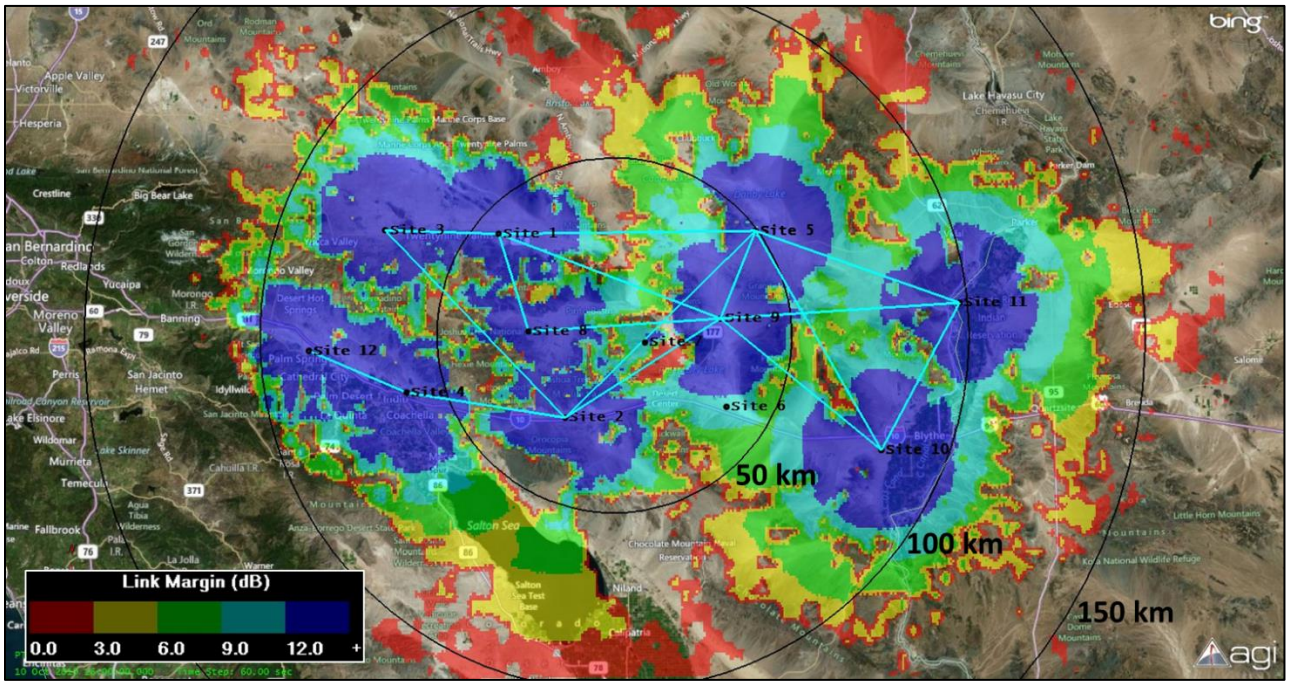

Figure 22. Architecture 13 for Radio A (Maximum Area Covered)

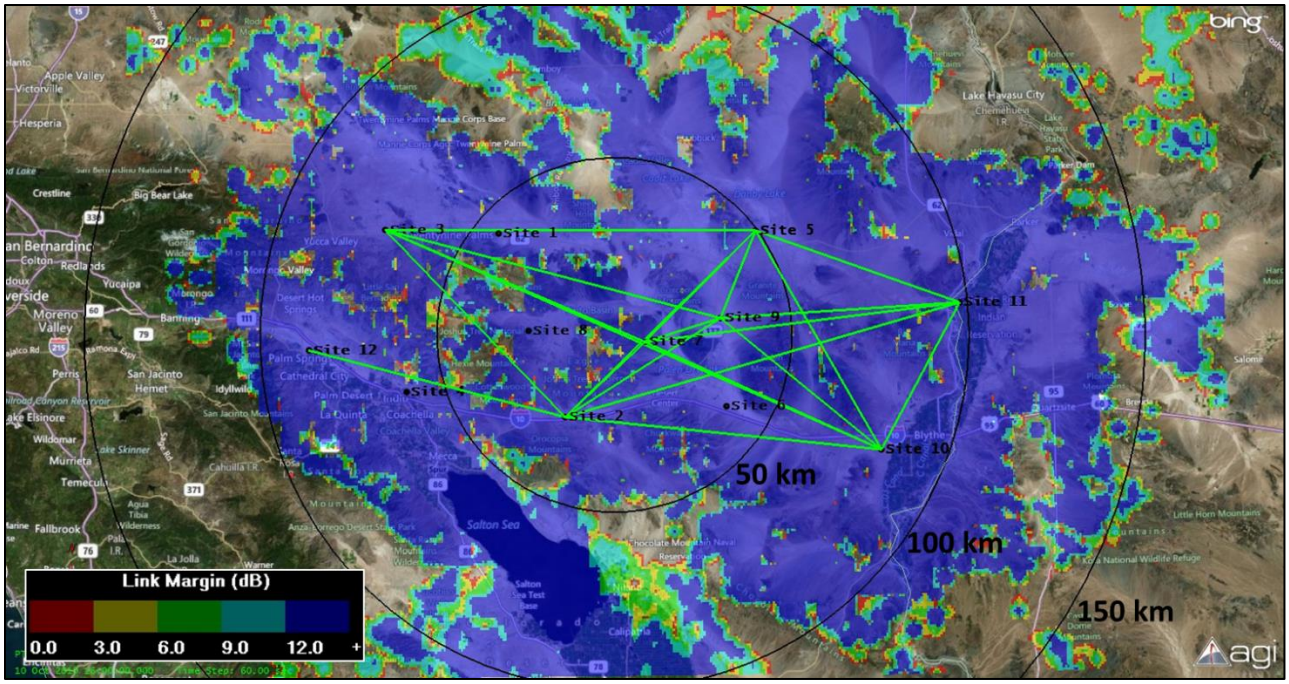

Figure 23. Architecture 8 for Radio B (Maximum Area Covered)

10.1.3 Radio Comparison for Balanced Architecture

The balanced architecture shows a robust topology for both Radio A and Radio B with no edge nodes that may be unreachable if a single node is not available and provides more coverage than the architectures presented in 10.1.1. Radio B offers a significant performance improvement in link performance and total area covered for only $800,000. This is a negligible increase given that the architectures both cost approximately $80 million. The consideration of a balanced architecture taken from the down-selected Pareto front can be useful for rapidly picking an architecture in the absence of a clear priority in the area covered and average number of crosslinks metrics.

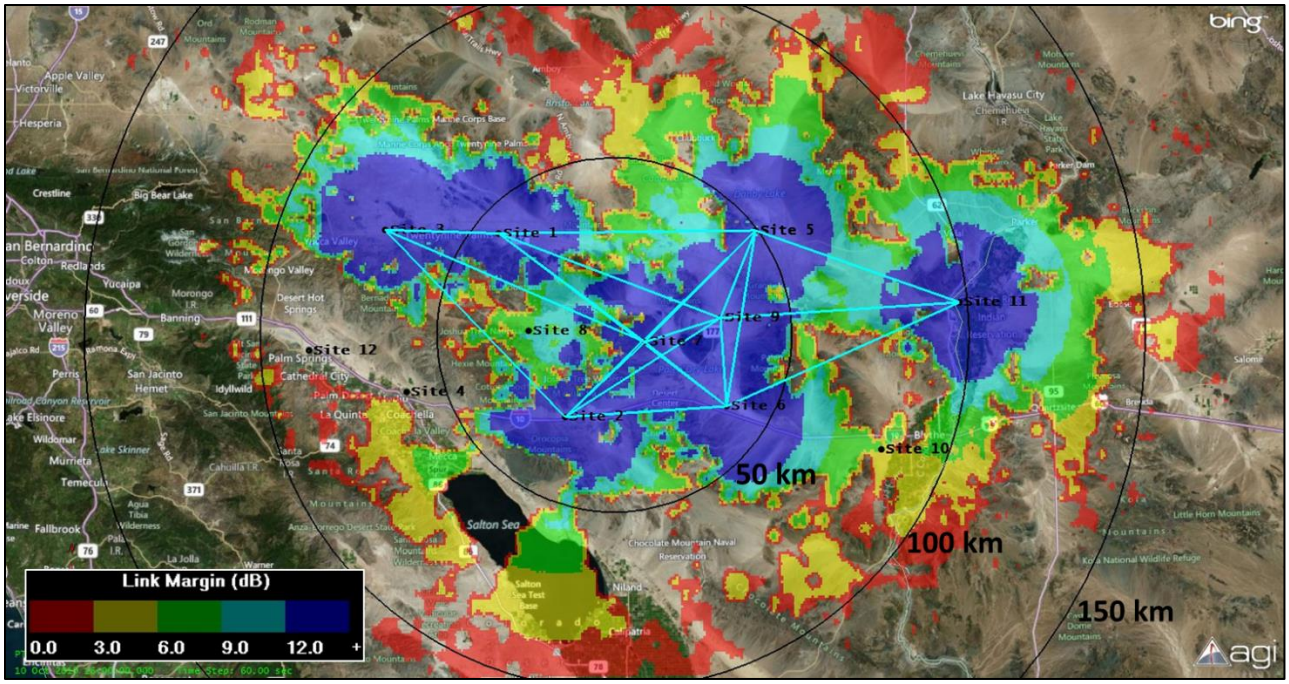

Figure 24. Architecture 12 for Radio A (Balanced Architecture)

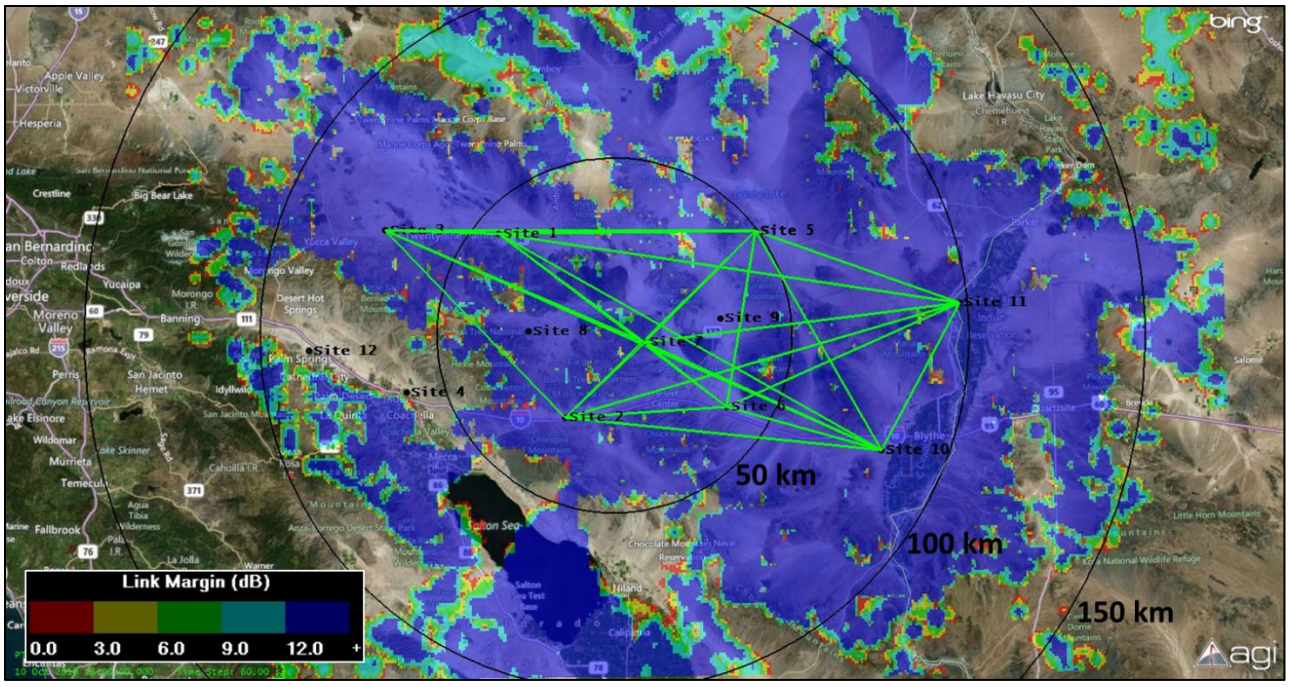

Figure 25. Architecture 9 for Radio B (Balanced Architecture)

10.2 Suitability of Site-to-Site Connectivity as a Measure of Network Resilience

The site-to-site connectivity matrix is utilized to evaluate the average number of cross-links for a given candidate architecture in the MOO. This performance metric is a measure of both throughput performance in the presence of relays and network resilience to the loss of nodes. Network resilience is relevant to decision makers because aircraft are unlikely to have 100% availability. Various factors such as maintenance and weather prevent the launch and execution of missions conducted by aircraft. In [21], Burke presents aggregate data for Air Force aircraft illustrating the percentage of time in given year that aircraft are mission capable (MC). These annual rates reveal MC rates between 70% - 80% which can degrade the performance of the network in providing connectivity between aircraft.

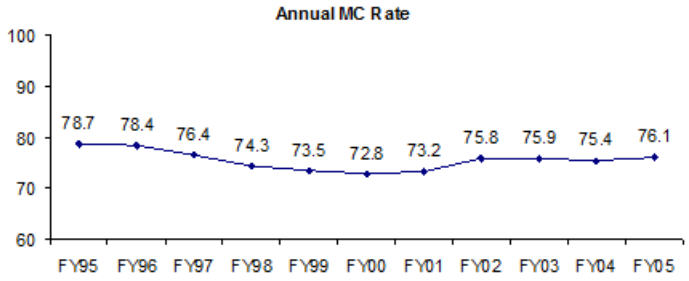

Figure 26. Aggregate Air Force Fleet Rates for Mission Capability [21]

To evaluate the utility of average number of crosslinks as a measure of network resilience, we can analyze two of the final candidate architectures for Radio A. The architectures to be analyzed will be the architecture maximizing ground coverage (with the lowest average number of crosslinks) and the architecture maximizing average number of crosslinks. From these two architectures, simulations can be conducted based on the MC rates presented in Figure 26 and network measures can be calculated to understand the degradation as aircraft are removed.

10.2.1 Analysis of Average Crosslinks in the Presence of Node Failures

While maximizing average number of crosslinks offers some measure of network performance, this measure can get skewed by certain sites exhibiting a higher number of average crosslinks. These “hub” nodes can mask the presence of edge nodes with a small number of crosslinks. Additional network measures are described in 11.3 that utilize a more holistic measure of network resilience from the perspective of minimizing the variance in average number of crosslinks to minimize hub nodes. Given the desire to maximize point to point connectivity for throughput performance, average number of crosslinks is a sufficient measure of network performance for this analysis. To illustrate the suitability of average number of crosslinks as a measure of network resilience, we can examine the decrease in average number of crosslinks as nodes are randomly removed from the architecture based on representative data for the MC rates of nodes.

Using MATLAB, we can randomly drop out nodes from the network based on the MC rate. A random number (drawn uniformly on the interval 1 to 100) will be generated for each node. If this random number exceeds the MC rate utilized for a given run, the node will be removed from the network. Note that for this analysis, it is assumed that individual aircraft being incapable of executing a given mission are independent events, which may not be true for specific platforms with known reliability issues or common failure modes. The resultant architecture will be combined with the previously calculated site-to-site connectivity matrix to extract the new topology with MC nodes. MC rates of 60%, 70% and 80% will be examined below to illustrate the degradation for various MC rates. These simulations will be useful for evaluating network resilience of the final architectures being considered for the deployment.

For the two architectures, 100 trials will be conducted and the average number of island nodes and edge nodes will be calculated. Island nodes are defined to be nodes in the network that are MC, but have no neighbors. The occurrence of island nodes in a given topology are important to quantify as this measure quantifies the event that an aircraft can operate on a given mission but cannot communicate with any other aircraft. Edge nodes are defined to be MC nodes with a

single neighbor. Understanding the number of edge nodes can provide insight into the number of occurrences of aircraft that can support the mission, but can only communicate with a single aircraft. These edge nodes will see a reduction in throughput to other sites as they will be forced to relay through their one neighbor.

An example output of a network with a 100% MC rate for the maximum ground coverage architecture for Radio A is shown below. Note that this topology matches what is shown in Figure 22.

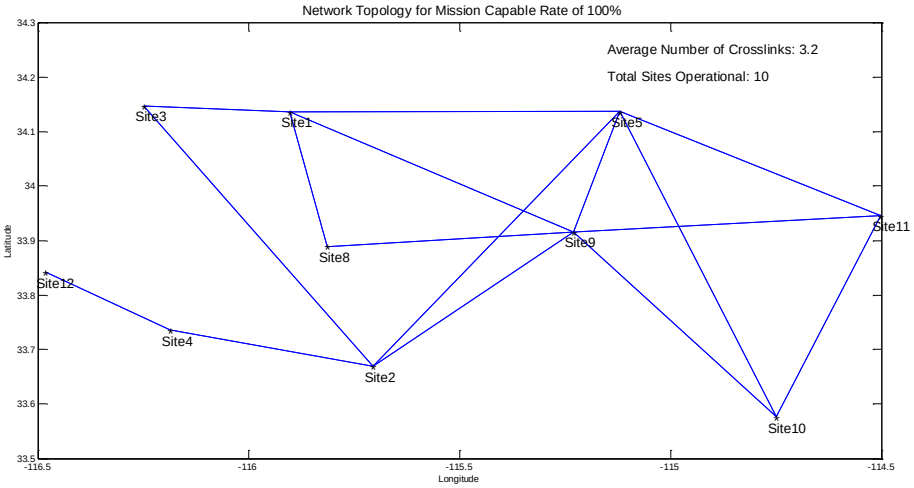

Figure 27. Example Network Generated in MATLAB

The network topologies in these runs will vary based on link closure probabilities and the loss of nodes, which can degrade the network. An example degraded network is shown in Figure 28. In this example network, Sites 3, 4, and 10 are edge nodes with only one neighbor. Site 8 is an island node with no neighbors.

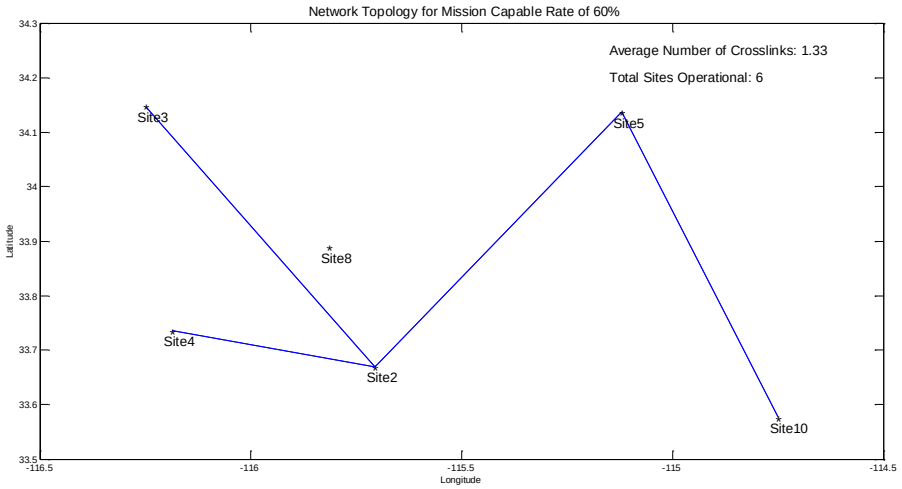

Figure 28. Example Degraded Network

Results

The results of the 100 trials for the three MC rates analyzed are summarized in Table 17. For the three MC rates analyzed, we see a large percentage of networks containing island nodes for the "Max Area Covered" architecture. For this architecture, 41% of the networks simulated contain at least one island node for the MC rate of 60% versus only 7% for the "Max Site to Site Connectivity" architecture. Even at MC rates of 80% (which is slightly optimistic based on the MC rates presented in Figure 26), the "Max Area Covered" architecture shows 29% of the networks containing at least one island node versus only 1% for the "Max Site to Site Connectivity" architecture. In addition, the higher number of crosslinks results in fewer networks with edge nodes. These simulation results reveal a clear indication that the average number of crosslinks metric provides higher network performance with respect to these metrics in the presence of node failure.

Table 17. Simulated Network Performance Metrics

Architecture	MC Rate	Average Crosslinks (100% MC Rate)	Simulated Average Crosslinks (100 trials)	Number of Trial Networks with Island Nodes	Number of Trial Networks with Edge Nodes
Max Area Covered	60%	3.2	1.8	41	91
Max Site to Site Connectivity	60%	5.4	2.8	7	41
Max Area Covered	70%	3.2	2.1	32	87
Max Site to Site Connectivity	70%	5.4	3.4	2	24
Max Area Covered	80%	3.2	2.5	29	83
Max Site to Site Connectivity	80%	5.4	4.1	1	16

A graph of island nodes for each MC rate is shown in the figures below. For the 60% MC rate, of the 7 occurrences of island nodes for the “Max Site to Site Connectivity” architecture, only one of these occurrences exhibits 2 island nodes. For the “Max Area Covered” architecture, we can observe multiple occurrences of 2 or more island nodes, indicating a large number of aircraft that cannot communicate.

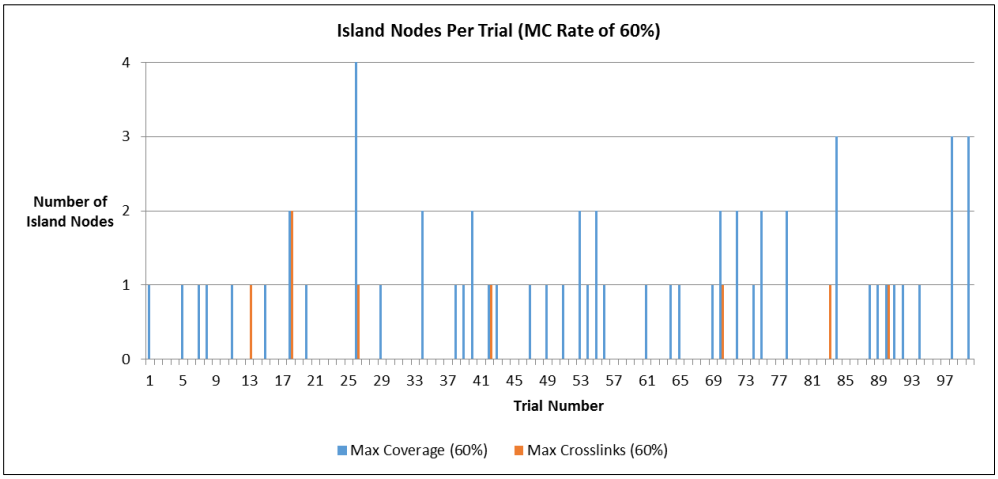

Figure 29. Island Nodes for 100 Trials (MC Rate of 60%)

For the MC rate of 70%, we see a drop off in the number of occurrences of 3 or 4 island nodes in the “Max Area Covered” architecture, but numerous cases with at least one island node. Conversely, we see only two occurrences of island nodes for the “Max Site to Site Connectivity” architecture.

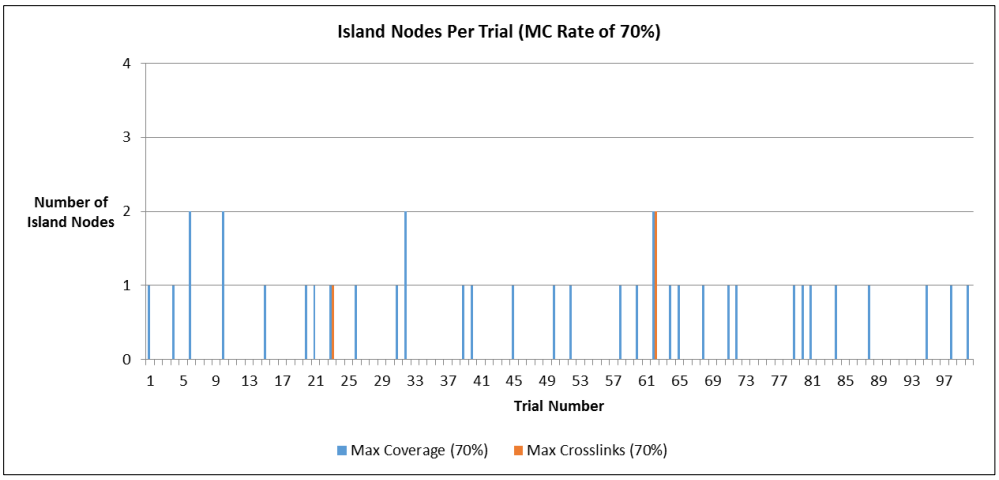

Figure 30. Island Nodes for 100 Trials (MC Rate of 70%)

The MC rate of 80% represents the most optimistic case for MC rates, yet numerous networks occur with at least 1 island node for the "Area Covered" architecture. In this trial, only 1 network with an island node is observed for the "Max Site to Site Connectivity" architecture.

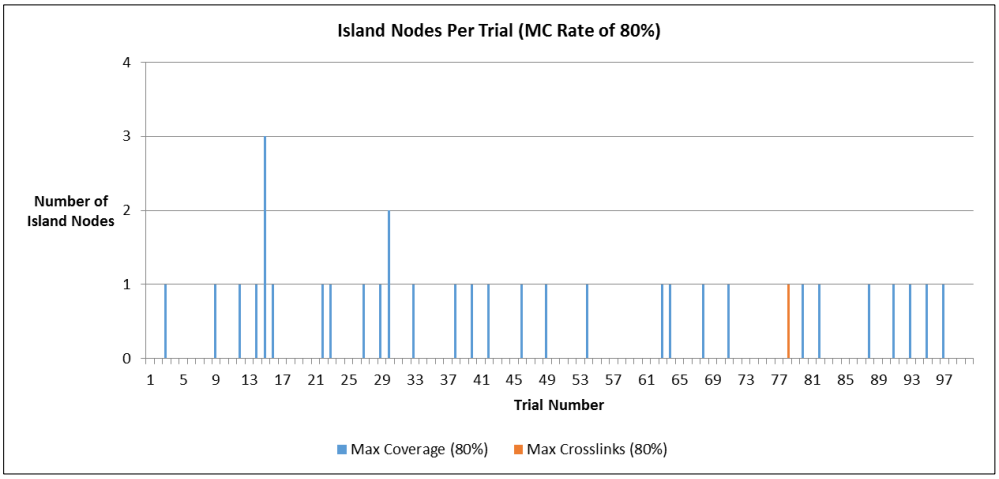

Figure 31. Island Nodes for 100 Trials (MC Rate of 80%)

From the simulations presented above, we can infer that the average number of crosslinks metric utilized for the architecture evaluation provides a useful measure of network performance in the presence of node failures. The "Max Site to Site Connectivity" architecture shown to have an average of 5.4 crosslinks per node appears to provide high tolerance against the loss of individual nodes for the MC rates considered. Decision makers can consider the

analysis presented here to understand the degradation in network performance for candidate aircraft with MC rates below 100%. While the tolerance for island nodes in the deployed networks depends on the nature of missions being conducted with the communications architecture, consideration of network resilience is important to understanding the expected performance of the selected architecture.

11 Future Extensions

This analysis could be extended to incorporate additional performance measures or modified objective functions to better differentiate performance of communications systems and model aircraft. Extensions for both are discussed below along with techniques for modifying the STK and MOO model to implement such extensions.

11.1 Dynamic Aircraft

The STK model assumes that the aircraft utilized have the ability to loiter in a fixed position at the stated altitudes for the duration of the scenario. This assumption simplifies the analysis in that performance degradation due to mobility of aircraft is not examined. Aircraft traveling along flight paths servicing ground nodes can induce outages of wireless links during banking or turn maneuvers, as antennas become masked by the aircraft body, preventing link closure. STK allows the definition of flight profiles for aircraft being modeled as well as body mask profiles for antennas, so aircraft could be extended to fly prescribed orbits to evaluate link performance over an appropriate time horizon and examining connectivity.

For performance analysis of radio links to ground users, the measure of performance could be modified to calculate average link margin over the time horizon being analyzed in lieu of the maximum link margin that is calculated in the current model. Additionally, this metric could be changed to examine “percent connectivity” which would measure the percent of time a ground node placed at the various grid points can successfully close a link. This same metric could be utilized for site-to-site connectivity between dynamic aircraft.

Extending the STK model to include dynamic aircraft will allow additional candidate aircraft to be considered in the MOO model and allow more flexibility in designing candidate architectures. However, adding dynamic aircraft operating over prescribed orbits would increase the processing time for enumerating the trade space and should be factored in to the architectural evaluation.

11.2 Adaptive Data Rates

Many tactical radios deployed to military users will provide adaptive data rates for throughput depending on the received signal level (RSL). As RSL decreases, throughput will typically degrade as radios attempt to send data at a lower rate which requires less signal power for successful link closure. The link margin metric utilized could be extended such that regions of link margin could map to throughput rates on candidate radios and an average throughput performance measure could be introduced to better differentiate performance of candidate radios. For example, for Radio B was stated to be 10 Mbps. If we assume that the radio adapts its data rate based on link margin (which can be combined with the known receiver sensitivity) based on the following table, average throughput can be calculated:

Table 18. Example Adaptive Data Rate RSL Thresholds

Link Margin (dB)	Data Rate (Mbps)
Greater than 10	10
6 – 10	5
3 – 6	1
0 – 3	0.5

Such a measure of performance could increase the level of fidelity for evaluating candidate radios that offer comparable throughputs and link ranges. A weighted sum of the link margins at each grid point, weighted by throughput, could offer an insightful metric of the throughput estimated for a given aircraft and ground node.

11.3 Network Topology Optimization

While important features of the network topologies desired by stakeholders in this architectural evaluation are not articulated, several metrics exist that could be leveraged in the evaluation. In [12], several network metrics are presented that could be leveraged to better understand the performance of the network topologies represented by the site-to-site connectivity matrices. These matrices are adjacency matrices weighted by the link margins calculated in STK, where connections between vertices (radio/aircraft pairs) are represented by non-zero link margins. The “degree” as defined in [13], is the number of links emanating from a

given node in the matrix, while a "path" is defined as the nodes that comprise in an indirect link between nodes not directly connected [13]. These features can be analyzed for given topologies to assess performance along these metrics.

In [12], centrality measures are presented that can be utilized to assess the robustness of a network to the loss of certain nodes. The candidate architectures presented rely on the availability of aircraft which have Aircraft 1 availabilities that are less than 100% of the time due to maintenance or weather. In the presence of the loss of nodes, network topologies could be analyzed based on the level of robustness to the loss of nodes through network centrality measures. In [12], "degree centrality ($C_D(t)$)" is defined as the number of degrees of a given node relative to the node with the highest degree:

$$C'_D(t) = C_D(t) / Highest\ Degree \tag{9}$$

The variance of the degree centralities could be leveraged to assess centralization at the network level. Values of degree centrality near 1 indicate the presence of highly central nodes, while values close 0 indicate decentralized nodes in the topology. Such a metric could be utilized to rank topologies of candidate architectures to assess tolerance to the loss of aircraft where architectures exhibiting the lowest network centralization being preferred.

In addition to the degree centrality measures, assessing average path lengths for network topologies could be an insightful metric. For a given topology, the average path length for all connections at a given site could be conducted over the entire candidate architecture to rank topologies by average path length. Such a measure could provide insight into how radio performance could be expected to degrade as information passes through multiple radio systems for transmitters and receivers not directly connected.

12 Conclusions

The intent of this architectural evaluation is to inform decision-making through the generation of the Pareto front for a large number of candidate architectures. The methodology developed and presented herein describes an approach for evaluating a large number of architecture combinations for representative tactical radio systems. The approach demonstrated the capability to down-select the architectural candidates from 531,441 combinations to three candidates for each radio type. From this set of six architectures, a detailed performance comparison can be conducted in support of an architectural recommendation. The approach provides an effective means of reducing the complex trade space to a tangible number of architectures to make an informed architectural decision. Furthermore, the analysis required only a high-level articulation of operational needs in the form of maximizing coverage area and site-to-site connectivity and the costs of aircraft and radio systems.

From these high-level needs, the enumeration of the trade space and generation of the Pareto front utilizing an MOO model can be conducted. Generation of the Pareto front can be quite valuable in aiding decision-makers in differentiating among candidate architectures. Down-selecting from the Pareto front and performing subsequent analysis on a handful of architectures raises important architectural questions that can aid in the articulation of more detailed requirements. For example, the presentation of the down-selected Pareto front in this evaluation provides an opportunity to prioritize delivering the communications system to certain sites with a greater operational need. In addition, from the down-selected Pareto fronts for Radio A and Radio B, a clear dominance in the selection of Aircraft 2 is evident. This feature of the Pareto front presents a need to understand the potential cost savings in utilizing only one aircraft from a lifecycle cost perspective.

The detailed evaluation of the remaining six architectures is made feasible by the down-selection of the Pareto front. While the down-selection in this analysis made some assumptions (picking the “best” architectures for site-to-site connectivity and total area covered, and picking the “balanced” architecture), the detailed analysis is made more manageable. Additionally, the

detailed analysis of only a small number of architectures allows stakeholders to gain additional insights, such as the tradeoff of area covered and site-to-site connectivity. A visual inspection of the topologies can be made to ascertain critical nodes in the topologies and potential requirements to offer coverage footprints around specific sites based on operational needs.

The power of the MOO model developed lies in the flexibility to tailor the model in the presence of new constraints. Generating the datasets for site-to-site connectivity and coverage area in STK is time-consuming, but the evaluation of the datasets in the MOO model is significantly faster. For the MOO evaluation of the two radio architectures, runtime for Radio A was approximately 46 minutes and runtime for Radio B was approximately 41 minutes on an Intel i5 processor-based laptop running Windows 8. The model can readily be modified to perform excursions in light of new constraints articulated by stakeholders. The addition of new candidate aircraft is straightforward, though it comes at an increased cost in the generation of STK outputs.

Extensions of the methodology presented can be developed in three key areas. First, the STK model and corresponding datasets generated can be modified to account for new aircraft types operating dynamic flight profiles. Metrics must be altered the account for the change in performance expected due to outages attributed to the changing geometry between aircraft to ground nodes. Additionally, link margin metrics could be extended to better model performance of candidate radio systems. Weighted throughput metrics could be incorporated that account for the change in performance as link margin changes. Lastly, if additional measures of network performance are articulated, network metrics could be used as a fitness function in the MOO model. These metrics could consist of average shortest path through nodes in the network or fault tolerance (measured by network centralization).

Appendix A – MATLAB Source Code

Source code for the MOO model is described below.

Multi Objective Decision Model Source Code

```
%Aircraft 1rchictures consist of one Aircraft 1t each site
nsites = 12;
%Aircraft 1 or 2 can be used at each site, requires 1x24 vector of decision
%variables for gamultiobj
nvars = 2*nsites;
radioA_cost = 50000;
radioB_cost = 150000;

%initialize ga options
%Set initial population (optional)
% InitPop = zeros(24,1);
% InitPop(22) = 1;
options      =      gaoptimset('InitialPopulation',InitPop','PopulationType',
'bitstring','PlotFcns',{@gaplotpareto});

%Read in ground coverage and site-to-site connectivity for Sites
rec_pwrA = csvread('C:\Users\Steve\Dropbox\Thesis\Complete Data Set\Radio A
Coverage.csv',1,0);
access_lmA = csvread('C:\Users\Steve\Dropbox\Thesis\Complete Data Set\Radio A
All Access (22 June 2013).csv',1,1);
rec_pwrB = csvread('C:\Users\Steve\Dropbox\Thesis\Complete Data Set\Radio A
Coverage.csv',1,0);
access_lmB = csvread('C:\Users\Steve\Dropbox\Thesis\Complete Data Set\Radio B
All Access (22 June 2013).csv',1,1);

%Run gamultiobj for Radio A using fitness function and 24 decision
%variables for aircraft/site combinations
ObjectiveFunctionA                              =                              @(arch)
Fitness_Function(arch,rec_pwrA,access_lmA,radioA_cost);
ObjectiveFunctionB                              =                              @(arch)
Fitness_Function(arch,rec_pwrB,access_lmB,radioB_cost);

%Store architectures and corresponding fitness functions for Pareto front
%of Radio A
[x_a,    fval_a,    exitflag_a,    output_a,    population_a,    scores_a]    =
gamultiobj(ObjectiveFunctionA,nvars,[],[],[],[],[],[],options);
%Store architectures and corresponding fitness functions for Pareto front
%of Radio B
[x_b,    fval_b,    exitflag_b,    output_b,    population_b,    scores_b]    =
gamultiobj(ObjectiveFunctionB,nvars,[],[],[],[],[],[],options);

%Dump Pareto fronts for each radio to csv file
csvwrite('Radio A GA Results.csv',[x_a fval_a]);
csvwrite('Radio B GA Results.csv',[x_b fval_b]);
```

Objective Function Source Code

```
function y = Fitness_Function(arch,rec_pwr,access_lm,radio_cost)

%calculate number of points where Link Margin is greater than 0
npoints = size(rec_pwr,1);
nvars = length(arch);
npgss = 0;
nptds = 0;
max_margin = zeros(npoints,1);
uniques = 0;

%Constraints cannot be applied to population types set to 'bitstring', so
%need to evaluate architecture and terminate if certain conditions arent'
%met

%Throw out candidates with two aircraft types at a single site by checking
%pairwise if Aircraft 1 and Aircraft 2 deployed to same site
k = 1;
while k < nvars
    if arch(k) == arch(k+1)
        y(1) = inf();
        y(2) = 0;
        y(3) = 0;
    end
    k = k + 2;
end

%If code gets to here, no candidate architectures with multiple aircraft
%at each site, calculate fitness functions

%calculate cost fitness function
for i= 1:nvars
    %if odd index, check for Aircraft 1
    if mod(i,2) == 1 && arch(i) == 1
        npgss = npgss + 1;
    elseif mod(i,2) == 0 && arch(i) == 1
        nptds = nptds + 1;
    end;
end;
y(1) = (5000000*npgss + 10000000*nptds) + (npgss+nptds)*radio_cost;

%Calculate unique coverage points for ground coverage fitness function
uniques = 0;
max_rsl = 0;
temp_mat = zeros(1,nvars);
for i=1:npoints
    temp_mat = arch .* rec_pwr(i,:);
    max_rsl = max(temp_mat);
    if max_rsl > 0
        uniques = uniques + 1;
    end
end

y(2) = -uniques*7.22;
```

```
num_links = 0;
num_aircraft = 0;
single_site_access = zeros(nvars,1)';
%Count number of site to site accesses for a given architecture
%note that current weighting is biased towards advantaged sites
%possibly restore architecture constraints
for j = 1:nvars
    if arch(j) == 0
        continue;
    else
        %count number of aircraft in candidate architecture
        num_aircraft = num_aircraft + 1;
        %only count accesses for aircraft in current architecture
        single_site_access = arch .* access_lm(j,:);
        for k = 1:nvars
            if single_site_access(k) > 0
                num_links = num_links+1;
            end
        end
    end
end
y(3) = -num_links/num_aircraft;
```

Network Analysis Source Code

```
coordinates = csvread('Sites2.csv',0,0);
labels = textread('Labels2.txt','%s');
access_mat = csvread('Radio A Adjacency.csv',0,0);
%full_mesh = csvread('full_mesh.csv',0,0);
%access_lm = csvread('C:\Users\Steve\Dropbox\Thesis\Complete Data Set\Radio A
Adjacency (22 June 2013).csv',1,1);
%[a_rows a_cols] = size(net);

mc_rate = 60;
arch = ones(12,1);

%max crosslinks radio A
mcl_a = [1  0   0   0   0   0   0   0   0   1   0   1   0   1   0   1   0   1
0   1   0   1   0   0]';
mgc_a = [1  0   0   1   0   1   1   0   0   1   0   0   0   0   1   0   0   1
0   1   0   1   1   0]';

%performance data for mgc arch
crosslinks_mgc = zeros(100,1);
island_nodes_mgc = zeros(100,1);
edge_nodes_mgc = zeros(100,1);
nodes_mgc = zeros(100,1);
mgc_island = 0;
mgc_edge = 0;

%performance data for mcl arch
crosslinks_mcl = zeros(100,1);
island_nodes_mcl = zeros(100,1);
edge_nodes_mcl = zeros(100,1);
nodes_mcl = zeros(100,1);
mcl_island = 0;
mcl_edge = 0;

%rng(1);
for trial = 1:100
    %initialize starting networks before dropping out nodes
%     mcl_net = (mcl_a * mcl_a') .* access_mat;
%     mgc_net = mgc_a * mgc_a' .* access_mat;
    test_arch_mgc = mgc_a;
    test_arch_mcl = mcl_a;

    %Drop out nodes
    for i = 1:24
        r = randi(100);
        if r > mc_rate
            test_arch_mgc(i) = 0;
            test_arch_mcl(i) = 0;
        end
    end

    %Create sample networks for each arch
    test_net_mgc = (test_arch_mgc * test_arch_mgc') .* access_mat;
    test_net_mcl = (test_arch_mcl * test_arch_mcl') .* access_mat;
    [a_rows a_cols] = size(test_net_mgc);
```

```
    %Calculate Edge/Island Nodes
    for i=1:a_rows
        %If site is present in architecture, calculate node metrics
        if test_arch_mgc(i) == 1
            if sum(test_net_mgc(i,:)) == 0
                island_nodes_mgc(trial) = island_nodes_mgc(trial) + 1;
                mgc_island = mgc_island + 1;
                %dum = 'island1'
            elseif sum(test_net_mgc(i,:)) == 1
                edge_nodes_mgc(trial) = edge_nodes_mgc(trial) + 1;
                mgc_edge = mgc_edge + 1;
                %dum = 'edge1'
            end
        end
        if test_arch_mcl(i) == 1
            if sum(test_net_mcl(i,:)) == 0
                island_nodes_mcl(trial) = island_nodes_mcl(trial) + 1;
                %dum = 'island2'
                mcl_island = mcl_island + 1;
            elseif sum(test_net_mgc(i,:)) == 1
                edge_nodes_mcl(trial) = edge_nodes_mcl(trial) + 1;
                mcl_edge = mcl_edge + 1;
                %dum = 'edge1'
            end
        end
    end
    %Calculate average number of crosslinks
    total_crosslinks_mgc(trial) = sum(test_net_mgc(:))/sum(test_arch_mgc);
    total_crosslinks_mcl(trial) = sum(test_net_mcl(:))/sum(test_arch_mcl);
    nodes_mgc(trial) = sum(test_arch_mgc);
    nodes_mcl(trial) = sum(test_arch_mcl);
end

%Calculate Averages
ave_cl_mgc = sum(total_crosslinks_mgc)/trial
ave_island_mgc = sum(island_nodes_mgc)/trial
ave_edge_mgc = sum(edge_nodes_mgc)/trial
ave_nodes_mgc = sum(nodes_mgc)/trial

ave_cl_mcl = sum(total_crosslinks_mcl)/trial
ave_island_mcl = sum(island_nodes_mcl)/trial
ave_edge_mcl = sum(edge_nodes_mcl)/trial
ave_nodes_mcl = sum(nodes_mcl)/trial

i_mgc = 0;
e_mgc = 0;
i_mcl = 0;
e_mcl = 0;

for count=1:100
    if island_nodes_mgc(count) > 0
        i_mgc = i_mgc + 1;
    end
    if island_nodes_mcl(count) > 0
        i_mcl = i_mcl + 1;
    end
    if edge_nodes_mgc(count) > 0
```

```
        e_mgc = e_mgc + 1;
    end
    if edge_nodes_mcl(count) > 0
        e_mcl = e_mcl + 1;
    end
end

i_mgc
i_mcl
e_mgc
e_mcl
% figure(1);
% gplot(test_net_mgc,coordinates,'-');
% %gplot(test_net,coordinates,'-');
% for j= 1:a_cols
%     if test_arch_mgc(j) > 0
%         text(coordinates(j,1) - .0058,coordinates(j,2) -
.0058,'*','FontSize', 16);
%         text(coordinates(j,1) - .02,coordinates(j,2) -
.02,labels(j),'FontSize', 14);
%     end
% end
% text(-115.15, 34.25, ['Average Number of Crosslinks: ', num2str(total1,3)],
'FontSize', 14);
% text(-115.15, 34.20, ['Total Sites Operational: ',
int2str(sum(test_arch_mgc))], 'FontSize', 14);
% title(['Network Topology for Mission Capable Rate of ',int2str(mc_rate),
'%'],'FontSize', 14);
% xlabel('Longitude');
% ylabel('Latitude');
% ylim([33.5 34.3]);
% xlim([-116.5 -114.5]);
```

Glossary

AGL	Above ground level
dB	Decibel
dBm	Decibel-milliwatts
DoD	Department of Defense
DTED	Digital terrain elevation data
FSPL	Free space path loss
GA	Genetic Algorithm
IP	Internet Protocol
km	kilometers
LOS	Line of sight
Mbps	Megabits per second
MHz	Megahertz
MOO	Multi-objective Optimization
MSL	Mean sea level
RF	Radio Frequency
RSL	Received Signal Level
RPA	Remotely-Piloted Aircraft
SATCOM	Satellite Communications
STK	Systems Toolkit
TIREM	Terrain Integrated Rough Earth Model

References

1. Welsh, Patty. "Colonel discusses vision of joint aerial layer network." *Hanscom Air Force Base - Home*. N.p., 8 Feb. 2013. Web. 18 May 2013. <http://www.hanscom.af.mil/news/story.asp?id=123335654>.
2. Marler, R.T., and J.S. Arora. "Survey Of Multi-objective Optimization Methods For Engineering." *Structural and Multidisciplinary Optimization* 26.6 (2004): 369-395. Print.
3. Winston, Wayne L., S. Christian Albright, and Mark Nathan Broadie. "Multi-Objective Decision Making." *Practical management science*. 2nd ed. Pacific Grove, CA: Brooks/Cole, 2001. 450-465. Print.
4. *Terrain Integrated Rough Earth Model (TIREM^{TM}) / Spherical Earth Model (SEM) Handbook* . McLean, VA: Alion Science and Technology, 2009. Print.
5. Rappaport, Theodore S.. "4." *Wireless communications: principles and practice*. 2nd ed. Upper Saddle River, N.J.: Prentice Hall PTR, 2002. 105-175. Print.
6. Sivanandam, S. N., and S. N. Deepa. *Introduction to genetic algorithms*. Berlin: Springer, 2007. Print.
7. Mitchell, Melanie. *An introduction to genetic algorithms*. Cambridge, Mass.: MIT Press, 1996. Print.
8. Holland, John H.. *Adaptation in natural and artificial systems an introductory analysis with applications to biology, control, and artificial intelligence*. Cambridge, Mass.: MIT Press, 1992. Print.
9. Deb, Kalyanmoy, Amrit Pratap, Sameer Agarwal, and T. Meyarivan. "A Fast and Elitist Multiobjective Genetic Algorithm: NSGA-II." *IEEE Transactions on Evolutionary Computing* 6.2 (2002): 182-197. *A Fast and Elitist Multiobjective Genetic Algorithm: NSGA-II*. Web. 30 June 2013.
10. "Global Optimization Toolbox - MATLAB." *MathWorks - MATLAB and Simulink for Technical Computing*. N.p., n.d. Web. 1 July 2013. <http://www.mathworks.com/products/global-optimization/index.html>.

11. "Use gamultiobj - MATLAB & Simulink." *MathWorks - MATLAB and Simulink for Technical Computing*. N.p., n.d. Web. 1 July 2013. <http://www.mathworks.com/help/gads/using-gamultiobj.html>.
12. Braha, Daniel. "Complexity in Project Organizations." System Project Management. MIT. MIT, Cambridge. 15 Nov. 2012. Lecture.
13. Monge, Peter R., and Noshir S. Contractor. "2." *Theories of communication networks*. Oxford: Oxford University Press, 2003. 29-41. Print.
14. Sanchez, M., Selva, D., Cameron, B., Crawley, E., Seas, A., Seery, B. "Exploring the architectural trade space of NASAs Space Communication and Navigation Program," *Aerospace Conference, 2013 IEEE* , vol., no., pp.1,16, 2-9 March 2013.
15. Ross, A.M., Hastings, D.E., Warmkessel, J.M., and Diller, N.P. "Multi-Attribute Tradespace Exploration as a Front-End for Effective Space System Design," *AIAA Journal of Spacecraft and Rockets*, Jan/Feb 2004.
16. Butler, R.K.; Creech, L.C.; Anderson, Albert J., "Considerations of Connecting MANETs Through an Airborne Network," *Military Communications Conference, 2006. MILCOM 2006. IEEE* , vol., no., pp.1,7, 23-25 Oct. 2006.
17. Cameron, B., Crawley, E., Selva, D. *Chapter X computational system architecture v2 DRAFT*. N.d. TS. MIT, Cambridge.
18. Schiavone, L.J., ""Airborne networking - approaches and challenges"," *Military Communications Conference, 2004. MILCOM 2004. 2004 IEEE* , vol.1, no., pp.404,408 Vol. 1, 31 Oct.-3 Nov. 2004.
19. Brand, J.; Bach, R., "Overcoming stressed satellite networks using alternative communications," *Military Communications Conference, 2009. MILCOM 2009. IEEE* , vol., no., pp.1,6, 18-21 Oct. 2009.
20. Bo Niu; Haimovich, A.M., "Optimal throughput of two-hop relay networks with different relay cooperation," *Military Communications Conference, 2009. MILCOM 2009. IEEE* , vol., no., pp.1,5, 18-21 Oct. 2009.
21. Burke, Christopher. "Operational Based AF Maintenance Standards. 2007. *Microsoft Powerpoint* file.